

FRET events in fluorescent pentapeptides containing aliphatic triazolo amino acid scaffolds: Role of spacer lengths

Subhendu Sekhar Bag*, Afsana Yashmeen

Bioorganic Chemistry Laboratory, Department of Chemistry, Indian Institute of Technology, Guwahati 781039, India



ARTICLE INFO

Keywords:

FRET efficiency
Spacer length
N-terminus flexibility
Aliphatic amino acid scaffolds
 β -Sheet pentapeptides

ABSTRACT

The FRET efficiencies in donor/acceptor pairs in the two termini of designed fluorescent pentapeptides depend on the flexibility of two arms of triazolyl amino acid scaffolds positioned in the center of the backbones inducing predominant β -sheet conformations. Flexible N-Terminus of the scaffold in a pentapeptide has led to higher FRET efficiency and makes it different from other peptide with flexible C-terminus.

1. Introduction

Förster resonance energy transfer (FRET) is an energy transfer phenomenon between a donor and an acceptor chromophore in a sufficient proximity (10–100 Å). In general, the donor and the acceptor with an overlapped emission and excitation spectra participate in FRET process [1]. The efficiency of this energy transfer is inversely proportional to the sixth power of the distance between donor and acceptor. A small change in this distance is reflected in FRET efficiency. Thus, FRET efficiency is widely used as a research tool in the field of chemistry, biology, biomedical research and in today's drug discovery [2]. FRET is one of few tools available for measuring the fluctuations in nanometer scale distances both *in vitro* and *in vivo* [3]. Due to its sensitivity, FRET has been used to investigate molecular level interactions [2] and to measure the end-to-end distances [4].

One common donor-acceptor FRET pair in biology used is a cyan fluorescent protein (CFP) – yellow fluorescent protein (YFP) pair [5]. In biology, FRET has been utilized to study the conformational changes of short polypeptides upon phosphorylation [6]. Recently, Iqbal et al. described the importance of fluorophore orientation for understanding FRET event in terms of distances in some circumstances in nucleic acid based scaffold [7a]. They showed Förster distance calculation resulted in an error upto 12 Å while considering the κ^2 value of 2/3. However, increasing the flexibility of the chain containing the fluorophores can diminish this discrepancy. The impact of heterogeneity on the FRET process was demonstrated by Vogel et al. using Monte Carlo simulations [7b]. The FRET is dependent on the relative orientation of transition dipoles of the donor and acceptor and their separation vector (κ^2). It was suggested that the isotropically or pseudo-isotropically random

orientation lead to low probability for FRET. However, under rapid isotropic sampling a dynamic random average value of 2/3 for κ^2 would lead to larger probability of FRET. On the same line, very recently, the importance of the differences in transition dipole orientation angle in donor-acceptor pair which is again dependent on the local micro-environment on the quantification of FRET process has been demonstrated by Bain and coworkers [7c].

Many more results and designed chromophoric pairs have been reported aiming at uncovering the structure, function, dynamics and interactions involving biomolecules inside a cell [8]. However, a number of issues need to be considered while designing an efficient FRET system, such as-(a) close proximity and (b) enough spectral overlap among donor/acceptor pairs. Moreover, the factors such as concentration, cellular localization etc. also played an important role in controlling the FRET process in biological systems. Therefore, design of an efficient FRET pair as well as their proper placement within a molecular entity is crucial in deciphering the bimolecular conformations.

2. The concept

Based on our earlier concept of design of peptidomimetic scaffolds, we thought that altering the length of amine (**m**) or acid terminus (**n**) or both, the triazolyl aliphatic amino acid scaffold (**A**) in a peptide backbone could induce β -sheet conformations (**B**) with varying propensities (Fig. 1) [9]. Furthermore, we envisioned that the extents of photo-physical dipolar interaction, such as, FRET, between two fluorescent amino acids (${}^{\text{TMnap}}\text{Ala}^{\text{Do}}$ and ${}^{\text{TPy}}\text{Ala}^{\text{Do}}$) at the two termini of pentapeptides would be different due to different spacer lengths (Fig. 1). Therefore, we would be able to establish a novel concept of distance

* Corresponding author.

E-mail address: ssbag75@iitg.ac.in (S.S. Bag).

<https://doi.org/10.1016/j.jphotochem.2019.04.024>

Received 23 January 2019; Received in revised form 14 April 2019; Accepted 16 April 2019

Available online 27 April 2019

1010-6030/ © 2019 Elsevier B.V. All rights reserved.

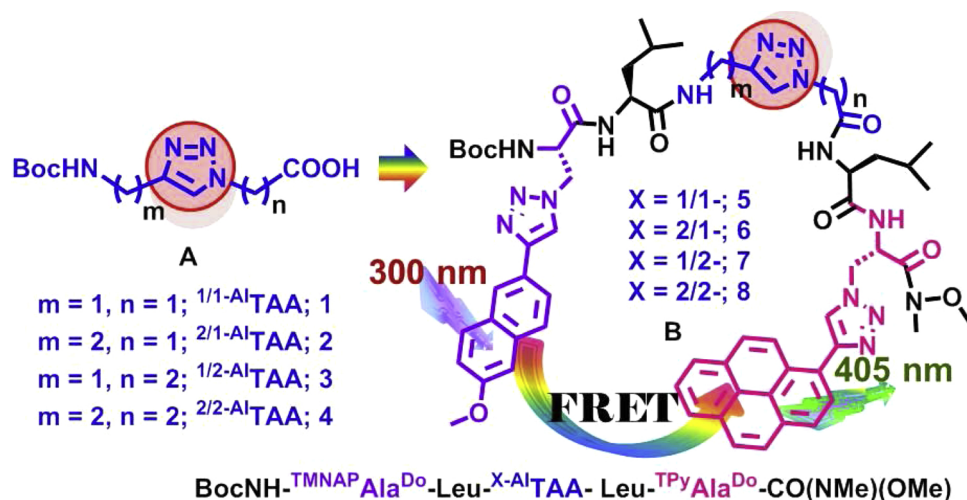


Fig. 1. Graphics of aliphatic triazolo amino acid scaffolds with different spacer lengths (A), the designed fluorescent pentapeptides (B) and the possible FRET event.

dependent FRET process in these designed peptides. Thus, with this concept, we planned to synthesise triazolyl amino acid scaffolds A of arm length differed by 1–2 carbon atoms on both N- and C- termini as β -sheet inducers and to place in the middle of the backbones of designed four fluorescent pentapeptides (Fig. 1).

Thus, we targeted to synthesise 1/1-, 2/1-, 1/2-, and 2/2-aliphatic triazolyl amino acid scaffold (1–4) having 1-carbon spacer in each terminus (1), 2-carbon spacer in N- and 1-carbon in C-terminus (2), 1-carbon spacer in N- and 2-carbon in C-terminus (3) and 2-carbon spacer in each terminus (4), respectively (Fig. 1). The scaffold 1 being the highest in rigidity and the scaffold 4 being the highest in flexibility constitute two extreme ends of our design. On the other hand, 2/1-scaffold 2 and 1/2-scaffold 3 are the two alternates in term of flexibility of N- and C-terminal arms, respectively. We expected that FRET efficiency would vary depending on the spacer length. Thus, the FRET efficiency would be higher and lower, respectively, at a largest and smallest spacer length maintaining the secondary structure. We, thus, established that increase in chain length of the scaffold enhances the extent of FRET efficiency which is due to increase in extent of flexibility that led to closeness of the donor/acceptor pair.

3. Results and discussion

3.1. The synthesis

The syntheses of aliphatic triazolyl amino acid scaffolds were started via Cu(I) catalyzed azide-alkyne cycloaddition (CuAAC) reaction following our earlier protocol [9]. Thus, the synthesis of 1/1-scaffold, 1, was reported earlier and we used the earlier synthesized material [9]. In short the synthesis was started from a conversion of ethyl bromoacetate (9) to ethyl azidoacetate (10) followed by click reaction with propargyl alcohol (11) following Scheme 1A. Subsequently the triazolyl alcohol 12 was converted to BocNH-triazolyl amino acid scaffold 1, (BocNH- ${}^{1/1}\text{AlTAA}$) in excellent yield (Scheme 1A). Next, the synthesis of scaffolds 2 was carried out starting with a click reaction between methyl 2-azidoacetate (17) and homopropargyl alcohol (18) following similar strategy. The click triazolyl product 19 was then subsequently transformed into triazolyl amino acid 23, (${}^{2/1}\text{-AlTAA}$) and then to scaffold 2 (BocNH- ${}^{1/1}\text{AlTAA}$) in excellent yield (Scheme 1B).

Following a similar strategy, we synthesized other two triazolyl amino acids 30 and 35 from where the BocNH-protected scaffolds 3 (BocNH- ${}^{1/2}\text{-AlTAA}$) and 4 (BocNH- ${}^{2/2}\text{-AlTAA}$), respectively, in very good yields (Scheme 2A–B).

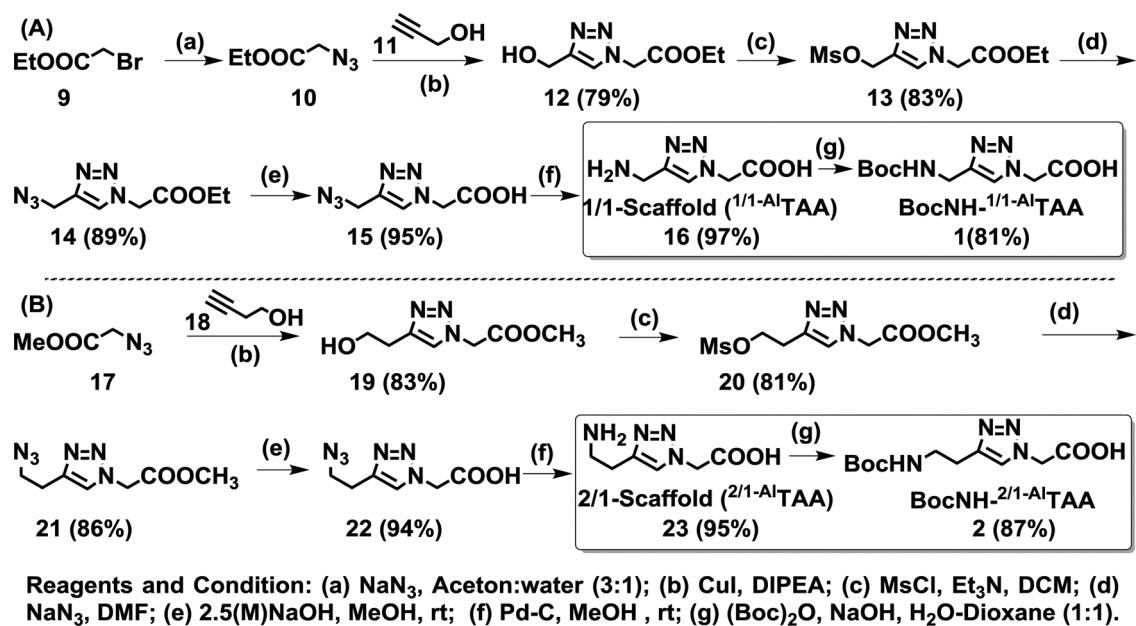
Next, the fluorescent pentapeptides with the scaffold amino acids

1–4 in the backbones were synthesized via the standard peptide coupling reaction following our earlier published protocol [9]. Thus, the synthesis of pentapeptide 5 [BocNH- ${}^{\text{TMNAP}}\text{Ala}^{\text{Do}}\text{-Leu-}{}^{1/1}\text{AlTAA}\text{-Leu-}{}^{\text{TPy}}\text{Ala}^{\text{Do}}\text{-CONMe(OMe)}$] containing ${}^{1/1}\text{-AlTAA}$ scaffold (1), was performed following Scheme 3A with 34% overall yield. The syntheses of other three unnatural fluorescent pentapeptides 6–8 containing aliphatic triazolyl amino acid scaffolds ${}^{2/1}\text{-AlTAA}$ (2), ${}^{1/2}\text{-AlTAA}$ (3) and ${}^{2/2}\text{-AlTAA}$ (4), respectively, of different spacer lengths were carried out using similar peptide coupling protocols (Schemes 3B for 6 and Scheme 4A–B for 7–8). All the intermediate and final peptides were purified by silica-gel (60–120 mesh) column chromatography and characterized with the help of analytical techniques such as, ${}^1\text{H}$, ${}^{13}\text{C}$ NMR and mass spectrometry.

3.2. Conformational analysis

Having our target peptides in hand, we, next, studied their conformations using various spectroscopic techniques. Thus, the secondary structure determination via circular dichroism (CD) spectropolarimeter of three fluorescent pentapeptides 5 and 7–8, containing aliphatic triazolyl amino acid scaffolds with different spacer lengths (1, and 3–4, respectively) in the backbone, showed predominantly β -sheet like structures (Fig. 2 and SI, Section 1) [10a–c]. The appearance of negative induced circular dichroism (ICD) bands in the chromophoric absorption region (300–350 nm) in all these peptides indicated the π - π stacking interactions between the two terminal chromophores (Fig. 2b, d) [10a–c]. The ICD correspond to triazolyl pyrene (TPy of ${}^{\text{TPy}}\text{Ala}^{\text{Do}}$) and triazolylmethoxynaphthalene (TMNAP of ${}^{\text{TMNAP}}\text{Ala}^{\text{Do}}$) absorptions appeared in the region of 345–378 nm (faint intensity) and at 287 nm (prominent intensity), respectively. The peptide 8 exhibited more intense ICD at 287 nm compared to 7 reflecting the role of more flexible spacer in peptide 8. On the other hand, the peptide 5 with rigid scaffold (1/1-spacer) possessed ICD bands of similar intensities.

The interesting CD spectrum was observed for peptide 6 which is different from other three peptides. Thus, in acetonitrile, it showed positive bands at 192 (weak), 200 and 218 nm indicating its extended helical conformation similar to poly-L-glutamic acid [10]. Moreover, the appearance of positive ICD bands at 290 and 305–365 nm are also indicative of a clear opposite characteristic feature of the peptide 6 compared to other three peptides (Fig. 2b, d). Interestingly, changing the solvent polarity from acetonitrile to MeOH, the peptide 6 showed a negative band at 192 nm and positive bands at 200 and 218 nm indicating its structural similarity to rat-tail collagen in the native state (SI, Fig. S1) [10]. On the contrary, in methanol all other three peptides, 5, and 7–8 behave in a similar way both in respect of CD as well as the

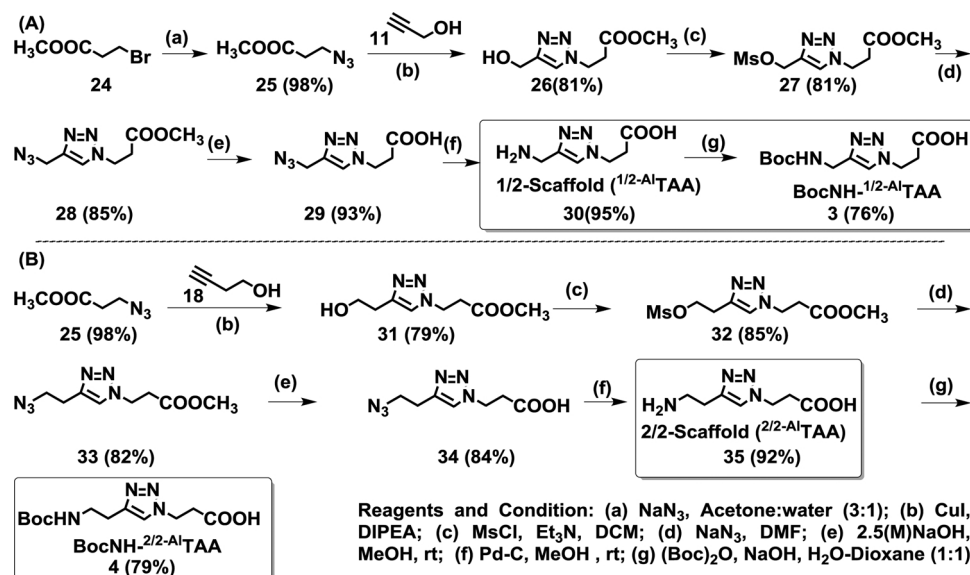
Scheme 1. Synthesis of aliphatic triazolyl amino acid scaffolds-(A) 1/16, $^{1/1}$ -AlTAA and (B) 2/23, $^{2/1}$ -AlTAA.

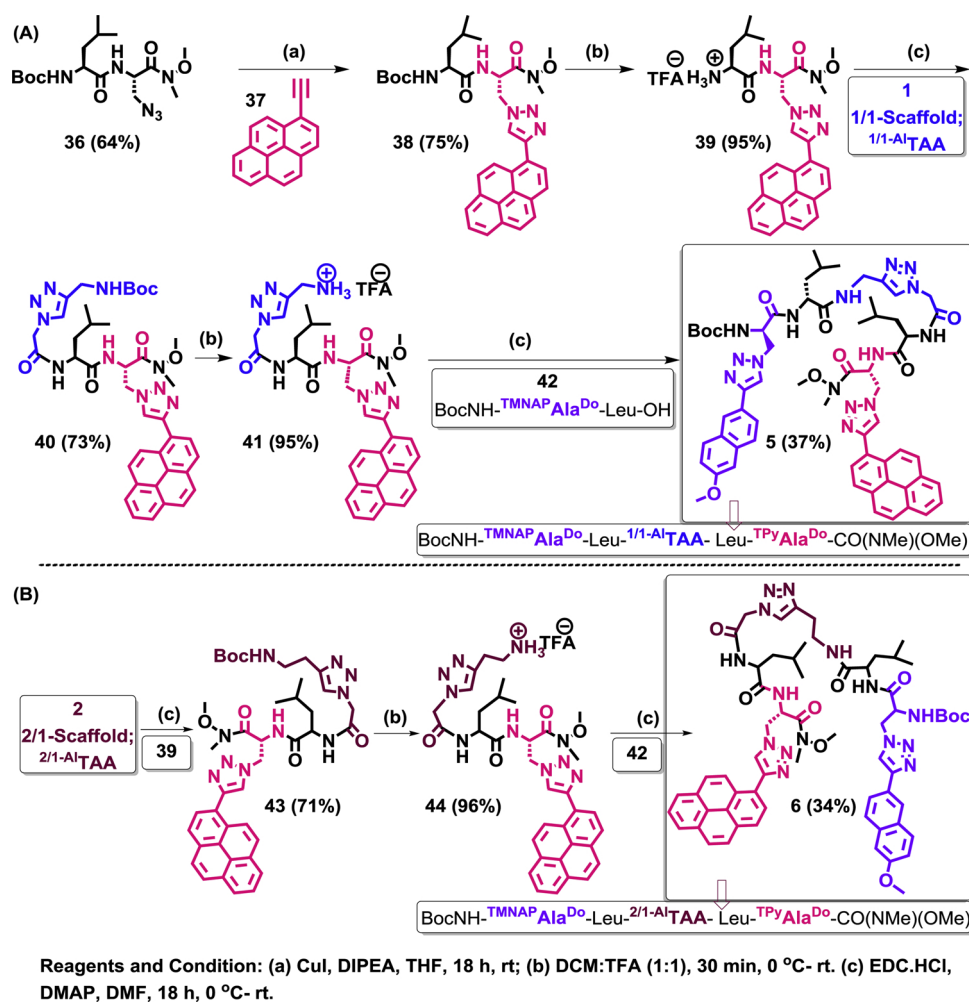
appearance of all positive ICD bands indicating more disorder structure in H-bonding solvent, methanol (SI, Fig. S1). These differences are reflecting the role of spacer length of the various scaffolds in these peptides (Fig. 1). More study is necessary to ascertain the effect of spacer length on the conformational rigidity which is our future target.

The H-bonded conformations were supported from IR and variable temperature NMR. Thus, the IR spectra showed the presence of intramolecular H-bonded and free amide -NH stretching absorptions at around $\bar{\nu} = 3310\text{--}3296\text{ cm}^{-1}$, C=O stretching at $\bar{\nu} = 1885\text{--}1660\text{ cm}^{-1}$ for all fluorescent pentapeptides, in particular, for peptides 5, 7 and 8 which supported β -sheet like structure [11]. VT-NMR analysis indicated the presence of weak intramolecular H-bonding between the two peptide strands (SI, Section 1.3) [11b]. In this experiment, a linear dependence of the change in chemical shift ($\Delta\delta$) of the protons involved in intramolecular H-bonding was observed with increase in temperature (T). Thus, the temperature coefficient ($\Delta\delta/\Delta T$) of the -NH proton is generally used to study the presence of intramolecular H-bonds [11b-d]. With increase in temperature, the -NH protons that are H-

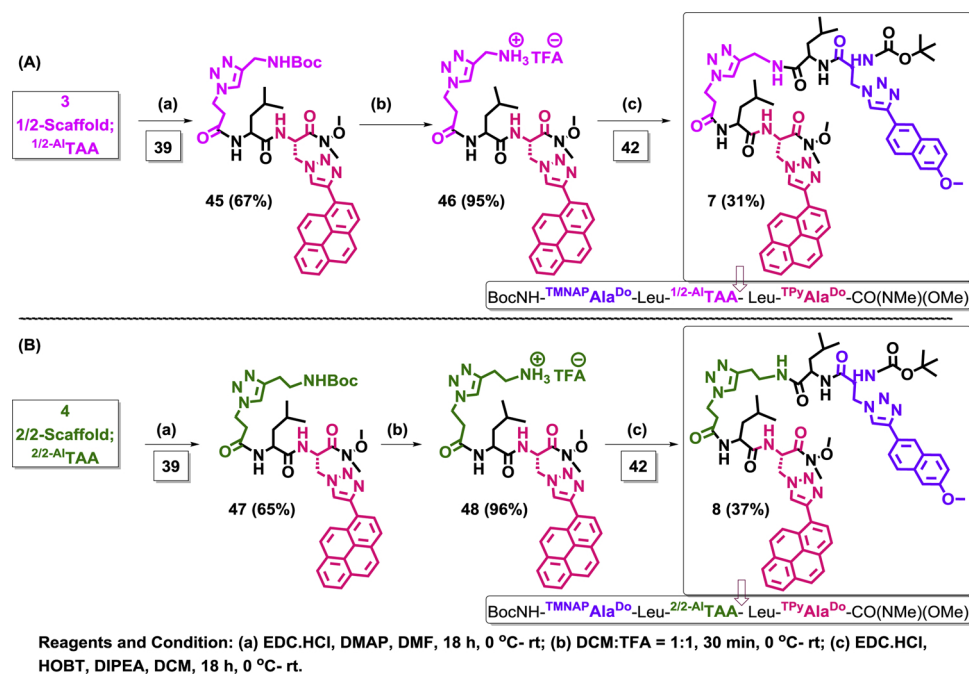
bonded intramolecularly exhibit upfield shifting of their resonance signals indicating the breaking of such intramolecular H-bonds. The temperature coefficients ranging from 0- (-)4.5 ppb K^{-1} are considered to be the indicator of strong intramolecular H-bonds [11b,c]. The values ranging upto (-) 8 ppb/k indicated the moderate to weak intramolecular H-bonds. A noticeable change in chemical shift was observed for the 2/1-scaffold-NH in peptide 6 wherein $\Delta\delta/\Delta T$ (-5.9 ppb/k) value was lowest among all amide-NHs of all peptides studied. This might be because of unique flexibility of the amino arm of the 2/1-scaffold containing two carbon spacer length at the N-terminus. This uniqueness was also reflected in the conformation adopted in CD by the peptide 6 having 2/1-scaffold in the backbone. Thus, both the CD and VT-NMR supported our design concept.

Next, the 2D NMR analysis in DMSO-d_6 was carried out to support the β -sheet conformation. The NOESY and ROESY spectra revealed the backbone H-bonding interactions indicating possible β -sheet conformations. The 2D NMR supported the close proximity of the two terminal fluorescent unnatural amino acids and possibility of a

Scheme 2. Synthetic scheme for the synthesis of two triazolyl aliphatic amino acid scaffolds-(A) $^{1/2}$ -AlTAA (30/3), and (B) $^{2/2}$ -AlTAA (35/4).



Scheme 3. Synthetic scheme for the fluorescent pentapeptides-(A) 5 and (B) 6 - containing scaffold $^{1/1}\text{-Al}^{\text{TAA}}$ (1) and $^{2/1}\text{-Al}^{\text{TAA}}$ (2), respectively, and fluorescent unnatural amino acids, $^{\text{TMNaP}}\text{Ala}^{\text{Do}}$ and $^{\text{TPy}}\text{Ala}^{\text{Do}}$.



Scheme 4. Synthetic scheme for the fluorescent pentapeptides-(A) 7 and (B) 8 - containing scaffold $^{1/2}\text{-Al}^{\text{TAA}}$ (3) and $^{2/2}\text{-Al}^{\text{TAA}}$ (4), respectively, and fluorescent unnatural amino acids, $^{\text{TMNaP}}\text{Ala}^{\text{Do}}$ and $^{\text{TPy}}\text{Ala}^{\text{Do}}$.

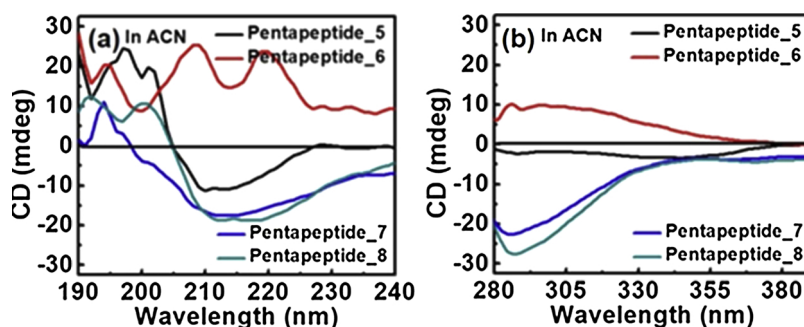


Fig. 2. (a) CD spectra of pentapeptides 5-8 in acetonitrile and (b) the ICD bands.

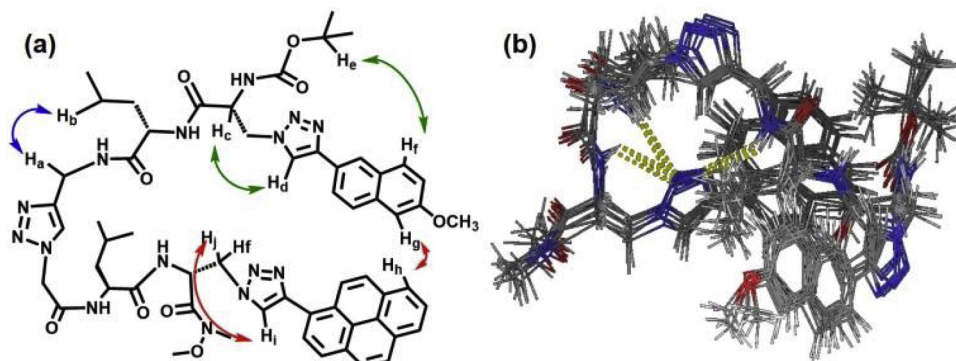


Fig. 3. (a) Schematics of long range ^1H - ^1H interactions in pentapeptide 5 as evident from 2D NMR and the (b) clustering of structures obtained from molecular dynamics simulation.

photophysical interaction between ($^{\text{TMNap}}\text{Ala}^{\text{Do}}$ / $^{\text{TPy}}\text{Ala}^{\text{Do}}$) for all pentapeptides [9b,c]. The possible observed interactions for one representative peptide 5 was shown in Fig. 3a. The MD simulations for the pentapeptides were carried out with Schrodinger MacroModel (Maestro vs. 9.1) software package using an OPLS 2005 force field which supported the β -sheet conformation (Fig. 3b) [12].

3.3. Photophysical property and FRET efficiency

The UV-vis and fluorescence photophysical properties of the fluorescent triazolyl amino acid monomers, $^{\text{TMNap}}\text{Ala}^{\text{Do}}$ and $^{\text{TPy}}\text{Ala}^{\text{Do}}$, (SI, Fig. S5-6; Table S3/4) indicated that there is a possibility of FRET process from donor $^{\text{TMNap}}\text{Ala}^{\text{Do}}$ to acceptor $^{\text{TPy}}\text{Ala}^{\text{Do}}$ in all peptides (SI, Fig. S11a). Furthermore, from the UV visible spectra of $^{\text{TMNap}}\text{Ala}^{\text{Do}}$ and $^{\text{TPy}}\text{Ala}^{\text{Do}}$ it was evident that at the absorption wavelength of $^{\text{TMNap}}\text{Ala}^{\text{Do}}$ ($\lambda_{\text{abs}}^{\text{max}} = 300 \text{ nm}$), the amino acid $^{\text{TPy}}\text{Ala}^{\text{Do}}$ absorb negligibly. Thus, it was clear that all the peptides 5-8 could selectively be excited at 300 nm.^{9a, d}

Upon excitation at the absorption maximum of the donor, $^{\text{TMNap}}\text{Ala}^{\text{Do}}$ ($\lambda_{\text{ex}} = 300 \text{ nm}$), the pentapeptide 5 showed a weak and overlapped emission at 365 nm corresponding to the emission from $^{\text{TMNap}}\text{Ala}^{\text{Do}}$ accompanied by another broad emission at 405 nm in all solvents (SI, Fig. S7, Table S5). The band at 405 nm is most expectedly the emission from TPy of $^{\text{TPy}}\text{Ala}^{\text{Do}}$ via FRET (SI, Fig. S11a-b). Fig. 4a clearly indicated that when the pentapeptide 5 was excited at 300 nm, the donor ($^{\text{TMNap}}\text{Ala}^{\text{Do}}$) fluorescence intensity decreased drastically while the acceptor ($^{\text{TPy}}\text{Ala}^{\text{Do}}$) fluorescence intensity increased from that of the bare acceptor. Thus, the steady state fluorescence clearly evidenced the FRET process in pentapeptide 5 (Fig. 4a). The occurrence of a FRET process was also evident from a time resolved fluorescence study. The lifetime measurements reveal complex excited state populations. Thus, the observed multiexponential fluorescence decays might be because of heterogeneous excited state population possibly arising out of either multiple emitting states or various molecular conformations, or noninteracting subpopulations of chromophores which is again

depends on local microenvironmental heterogeneity.⁷ The similar situations are quite frequent in most fluorescent proteins [13]. In summary, we observed a decrease in donor life time ($^{\text{TMNap}}\text{Ala}^{\text{Do}}$, $\lambda_{\text{ex}} = 290 \text{ nm}$, $\lambda_{\text{em}} = 365 \text{ nm}$) from 6.8 to 3.38 ns in pentapeptide 5 in acetonitrile (SI, Fig. S12a, Table S9) indicating a FRET process [9]. At this stage, the detailed investigation of the potential of the rise time of acceptor fluorescence to probe FRET was not done. In future, we would like to quantify the FRET from the rise time of acceptor fluorescence which should be equivalent to donor fluorescence lifetime [14].

Under the same experimental condition, other pentapeptide 6 also showed a weak emission at 365 nm corresponding to the emission from $^{\text{TMNap}}\text{Ala}^{\text{Do}}$ along with a broad emission at 405 nm (SI, Fig. S8, Table S6) when excited at the absorption wavelength of $^{\text{TMNap}}\text{Ala}^{\text{Do}}$ ($\lambda_{\text{abs}}^{\text{max}} \approx 300 \text{ nm}$). Similar to the case in peptide 5, when the pentapeptide 6 was excited at 300 nm, the donor ($^{\text{TMNap}}\text{Ala}^{\text{Do}}$) fluorescence intensity decreased drastically while the acceptor ($^{\text{TPy}}\text{Ala}^{\text{Do}}$) fluorescence intensity increased from that of the bare acceptor supporting a FRET process in pentapeptide 6 (Fig. 4b). The occurrence of FRET process was evident from a time resolved fluorescence study wherein we observed a decrease in donor life time ($^{\text{TMNap}}\text{Ala}^{\text{Do}}$, $\lambda_{\text{ex}} = 290 \text{ nm}$, $\lambda_{\text{em}} = 365 \text{ nm}$) from 6.8 to 3.15 ns in pentapeptide 6 (SI, Fig. S12b, Table S9). The FRET events in pentapeptide 7-8 were also evident both from steady state as well as from time resolved fluorescence study (SI, Fig. S9-10, Table S7-8 and Table S9-S10). However, the extents of intensities/efficiencies were different.

3.4. Flexibility and the FRET efficiency

We, next, turn our attention to investigate the cause of above differences. Is there any role of flexibility i.e. the length of the spacers in the scaffolds? Is there any role of flexibility to bring the FRET pair closer to each other? Spacer length of which terminus of the peptides 5-8 is more effective in bringing more flexibility and hence FRET efficiency? The analysis of relative steady state emission intensities of donor ($^{\text{TMNap}}\text{Ala}^{\text{Do}}$)/acceptor ($^{\text{TPy}}\text{Ala}^{\text{Do}}$) in a peptide and in their bare

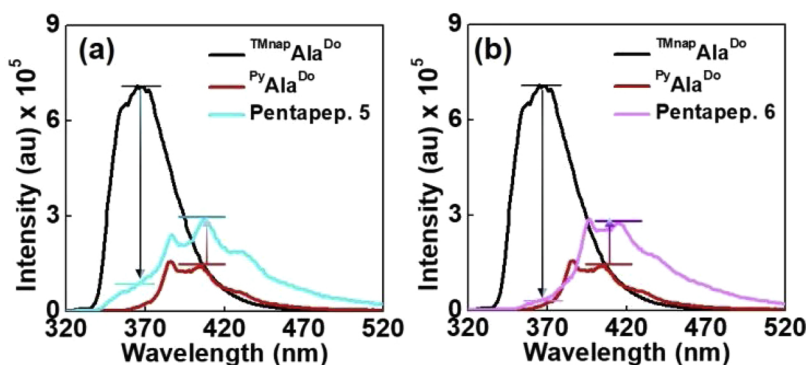


Fig. 4. Fluorescence spectra of individual donor amino acid, $^{TMnap}Ala^{Do}$, acceptor amino acid, $^{TPy}Ala^{Do}$ and (a) the pentapeptide 5 and (b) pentapeptide 6 ($10 \mu M$ each, r.t., $\lambda_{ex} = 300$ nm) in MeOH showing FRET process.

states along with the time resolved fluorescence study suggested that the extent of FRET process from $^{TMnap}Ala^{Do}$ to $^{TPy}Ala^{Do}$ in all the pentapeptides differed from each other. This might be because of the differential proximity of the two terminal chromophores which is again dependent on the length of the carbon spacer (no. of carbons) of C-/N-terminus of triazolyl amino acid scaffolds in the backbone of the peptides. As per our limited design, the spacer length is highest (two carbon distance) in case of 2/2-scaffold 4 (Fig. 1). Therefore, the two peptide arms are highest most flexible in case of pentapeptide 8 containing 2/2-scaffold 4 allowing the two chromophores in two termini to come to a closest distance compared to other peptides. This highest flexibility and closest positioning of the terminal donor/acceptor chromophores expectedly would result in highest extent of FRET in peptide 8 (SI, Fig. S12b) [7].

On the other hand, the 1/1-scaffold amino acid 1 is most rigid among all other scaffolds which expectedly would bring more rigidity on to the peptide arms. That means the two terminal chromophores would remain in a fixed and rigid distant away compared to other cases. This rigidity brought two donor/acceptor chromophores farthest away and expectedly would result in lowest extent of FRET in peptide 5 (SI, Fig. S12b). Conversely, 2/1-scaffold 2 containing peptide 6 and 1/2-scaffold 3 containing peptide 7 are the two alternates in term of flexibility of N-terminus and C-terminus arms, respectively, as well as in terms of closeness of two terminal chromophores. From the CD spectrum and VT-NMR study it was clear that the peptide 6 is unique in respect of conformational adaptation and intramolecular H-bonding interaction through scaffold-NH units (SI, Section 5). The more flexible nature of peptide 8 compared to peptide 7 and 5 was also reflected from an intense ICD band. Moreover, the opposite nature of the peptide 6 compared to other three peptides was also reflected in the ICD bands (Fig. 2b). Therefore, we expected that the CD spectral behaviour and the flexibility would be reflected in their corresponding FRET efficiency. The 2-C spacer length in the N-terminus led peptide 6 comparatively more flexible than peptide 7 with 1-C spacer length as was evident from more intramolecular H-bonding ability of scaffold-NH in peptide 6. Therefore, we would expect that the terminal donor-acceptor chromophores would be more close in peptide 6 than in peptide 7 which ultimately would lead to more FRET efficiency in peptide 6 [4–6].

The calculated FRET efficiencies in all the peptides exactly followed the above explanation establishing our concept of distance dependent FRET and the logic of design. The FRET efficiency was found to be highest for highest flexible pentapeptide 8 (96%), lowest for lowest flexible pentapeptide 5 (85%) and moderate for moderately flexible pentapeptide 6 (95%) and pentapeptide 7 (94%) (SI, Fig. S12). The results clearly suggested that the increased flexibility in terms of spacer length in the N-terminus has a more gross effect in enhancing the FRET efficiency compared to the C-terminus. This may be due to the increase of flexibility of the molecular scaffold to help getting turn in such a way

that two termini come close together and the extent of FRET increases. All these results supported our expectation and explanation on the flexibility in peptide and the extent of FRET. Thus, the hypothesis of increase in extent of FRET via increase in two terminal flexibilities along with our observations in the limited designs would be worthy of further investigation [7].

4. Conclusion

In conclusion, we have successfully synthesized aliphatic triazolyl amino acid molecular scaffolds of various spacer length and incorporated them into the backbones of designed fluorescent pentapeptides in order to achieve turn induced β -sheet fluorescent pentapeptides. We established a correlation among the spacer length of the two arms of the amino acid scaffolds, the extent of flexibility and the extent of FRET process among the two terminally situated FRET pairs. Our result suggested that the increase of flexibility of the molecular scaffold helps getting turn in such a way that two termini come close together and the extent of FRET increases. Our study might shed light to design of peptide-based molecular rulers to probe distance-dependent FRET processes.

5. Experimental section

5.1. General experimental

All reactions were carried out under inert atmosphere using flame-dried glassware. Combined organic layers were dried over anhydrous sodium sulfate. After work up solvents were removed in a rotary evaporator under reduced pressure. For column chromatography Silica gel (60–120 mesh) was used. Reactions were monitored by TLC on silica gel 60 F254 (0.25).

1H NMR spectra were recorded either at 400 MHz or at 600 MHz and ^{13}C NMR spectra were recorded either at 100 MHz or at 150 MHz (mentioned accordingly). Coupling constants (J value) were reported in hertz (Hz). The chemical shifts were shown in ppm downfield from tetramethylsilane, using residual chloroform ($\delta = 7.26$ in 1H NMR, $\delta = 77.23$ in ^{13}C NMR), DMSO ($\delta = 2.5$ in 1H NMR, $\delta = 39.5$ in ^{13}C NMR), as an internal standard. Mass spectra were recorded with a HR mass spectrometer and data analyzed by using built-in software. IR spectra were recorded in KBr on a FT-IR spectrometer. All 2D NMR Experiments were carried out on 600 MHz spectrometer at room temperature using 7–10 mM concentration in d_6 -DMSO solvent. Spectra were acquired with 2048×256 in both dimension (F2 and F1) and other parameter are given below. **TOCSY**: Free induction decay (FID) with NS = 16 and DS = 32, relaxation delay (D1) 2 s, mixing time (D9) 0.08 s, acquisition time (AQ) 0.085 s, spectral width 12,019 Hz. **ROESY**: Free induction decay (FID) with NS = 16 and DS = 16, relaxation delay (D1) 2 s, mixing time (P15) 0.02 s, acquisition time (AQ) 0.085 s,

spectral width (SWH) 12,019 Hz. **NOESY** : Free induction decay (FID) with NS = 8 and DS = 16, relaxation delay (D1) 2 s, mixing time (D8) 0.6 s, acquisition time (AQ) 0.085 s, spectral width (SWH) 12,019 Hz. **VT-NMR**: The presence of intramolecular H-bonds in the peptides was assessed through the variable temperature (VT) NMR by determining the variation of chemical shifts of the various -NHs with temperature (20 °C–75 °C) in d_6 -DMSO solvent.

5.2. Some general procedure for our synthetic scheme of pentapeptides

5.2.1. General procedure for the preparation of azide from bromo

To a solution of bromo compound (1 equiv.) in water/acetone (1:3) was added NaN_3 (1.5 equiv.) and the mixture was heated at 60 °C for 4 h. Then the reaction mixture was diluted with DCM and washed with water. The organic layer was dried over anhydrous Na_2SO_4 and concentrated in vacuum. The crude material was obtained in quantitative yield. This can be used for next step without further purification.

5.2.2. General procedure for [3 + 2] cyclo-addition (Click reaction)

The prepared azido compound taken in dry THF and degassed for 5 min with nitrogen gas. After adding alkyne (1.1 equivalent) degassing was continued for the next 5 min. Then 1 mol % powdered CuI was added. Then 1.2 equivalent DIPEA was added and reaction mixture was degassed and allowed to proceed for 18–20 h at room temperature. After total consumption of the starting azide, the reaction mixture was evaporated completely and work up was done by EtOAc and NH_4Cl solution. The organic layer was washed with brine, dried over Na_2SO_4 . The title triazolyl compound was separated by column chromatography and characterized.

5.2.3. General procedure for the preparation of mesyl derivative from hydroxyl group

In a dry R.B –OH compound (1 equivalent) was loaded in a dry CH_2Cl_2 . Mesyl chloride (1.4 equivalent) and triethylamine (1.3 equivalent) were added to the reaction mixture at 0 °C. The reaction mixture was stirred at 0 °C till the starting material was consumed. After that the reaction mixture was diluted with DCM and washed with water and dried over Na_2SO_4 and then evaporated in vacuum. The pure compound was then isolated by column chromatography and utilized immediately for the next step without further characterization.

5.2.4. General procedure for the deprotection of the methyl ester

To a solution of the respective methyl ester protected peptide in THF: H_2O = 5 : 1, lithium hydroxide (1.5 equivalent) was added at 0 °C. The reaction mixture was stirred for about 3–4 hour until starting material was fully consumed. Reaction was monitored by TLC. After completion of the reaction, solvent was dried by rotary evaporator. Then water (4–5 ml) was added to the reaction mixture and cooled to 0 °C. The dilute acetic acid was added to the reaction mixture to adjust pH- 3–4. The reaction mixture was extracted with EtOAc. The combined organic layers were dried over Na_2SO_4 . The hydrolyzed compound was isolated by column chromatography (Si-gel, CHCl_3 :MeOH = 10:1). Yield was 90–96%.

5.2.5. General procedure for the preparation of azide from mesyl derivative

To a solution of mesyl compound (1 equivalent) in dry DMF was added NaN_3 (1.5 equiv.) and the mixture was stirred at room temperature. Then the reaction mixture was diluted with DCM and washed with water. The organic layer was dried over anhydrous Na_2SO_4 and concentrated in vacuum. The product was isolated by column chromatography and characterized. Yield was 70–75%.

5.2.6. General procedure for the preparation of amine from azide derivative

To a solution of the azide compound in methanol Pd/C is added and to it hydrogen gas balloon was set and stirred the reaction mixture for

3–4 h. The solvent methanol was then evaporated and the crude mass was dissolved in water and then filtered, filtrate is evaporated to afford the compound with quantitative yield.

5.2.7. General procedure for the Boc protection of amine group

In a solution of amine compound (1 equivalent) in 1:1 mixture of 1,4 dioxane and water (3 ml each) was added NaOH (2 equivalent) followed by di-tert-butyl dicarbonate (1.5 equiv.) maintaining the pH between 7.5–8.5. The reaction mixture was stirred at room temperature for 20 h. The reaction mixture was washed with ethyl acetate (2 x 10 ml) and the aqueous phase was treated with dilute HCl to bring pH 4 in cold condition. Immediately the solution was extracted with ethyl acetate and the organic layer was washed with water, brine, dried and evaporated under vacuum to furnish the Boc-protected amine derivative as white solid in pure form.

5.2.8. General procedure for the Peptide coupling

To a solution N-protected amino acids in 3:1 mixture of dry DCM and DMF, 1-[3-dimethyl amino propyl]-3-ethylcarbo-diimide hydrochloride (EDC.HCl) (1.2 equivalent) and HOBT (1.2 equivalent) were added and the reaction mixture was stirred for 1 h at 0 °C. Then the amine salt of wienreb amide or methyl ester protected corresponding amino acids or dipeptide (1.1 equivalent) were added followed by diisopropylethylamine (DIPEA) (2.4 equivalent). The reaction mixture was stirred for another 18–20 h at 0 °C to room temperature. Then solvent was dried by rotary evaporator, after which it was partitioned between EtOAc and aqueous NaHCO_3 solution (50 ml each). The organic layer was washed with brine solution. Pure product was isolated by column chromatography.

5.2.9. General procedure for the deprotection of the Boc-group

The respective both side protected amino acids and peptides was dissolved in CH_2Cl_2 and cooled to 0 °C. TFA (equal amount as the solvent) was added and the solution was allowed to warm to room temperature. The stirring was continuing at room temperature until the starting material was consumed (monitored by TLC). The reaction mixture was evaporated in vacuum. The residual TFA was evaporated by triturating the mixture with dry toluene thrice, evaporated thrice and dried to afford the product in quantitative yield.

5.3. Synthesis of aliphatic triazolo amino acid scaffolds of various spacer lengths (1–4)

5.3.1. Synthesis of 1/1-Scaffold (1)

The synthesis of 1/1-scaffold (1, $\text{BocNH}^{-1/1}-\text{Al}^{\text{TAA}}$) was carried out following the **Scheme S1 A** and our earlier literature protocol and followed the following steps.

5.3.1.1. Synthesis of ethyl azido acetate (10): [8a,b]. To a solution of ethyl bromoacetate (9, 1510 mg, 9.04 mmol) in water/acetone (1:3) was added NaN_3 (881.6 mg, 13.56 mmol) and the mixture was heated at 60 °C for 4 h. Then the reaction mixture was diluted with DCM and washed with water. The organic layer was dried over anhydrous Na_2SO_4 and evaporated in vacuum. The crude material was obtained in quantitative yield. The product 10 is oily liquid. Yield 97%. IR (KBr) 2955, 2103, 1741, 1441, 1372, 1175, 1064 cm^{-1} . The azide was used for the next step without further purification and characterization.

5.3.1.2. Synthesis of ethyl 2-(4-(hydroxymethyl)-1H-1,2,3-triazol-1-yl) acetate (12): [8a,b]. This compound is known compound [8a,b]. The prepared ethyl azido acetate 10 (500 mg, 3.876 mmol) and propargyl alcohol 11 (0.246 ml, 5.8 mmol) was undergone click reaction to get the corresponding triazolyl alcohol compound. The title alcohol compound 12 was isolated by column chromatography (Si-gel, PE:EA = 1:1) in pure form as amorphous white solid (560 mg, Yield 79%). ^1H NMR (CDCl_3 , 600 MHz) δ 1.26 (3H, t, J = 3.0 Hz), 4.21 (2H,

q, $J = 5.4$ Hz), 4.74 (2H, d, $J = 7.8$ Hz), 5.10 (2H, s), 7.63 (1H, s). $^{13}\text{C}\{1\text{H}\}$ NMR (CDCl_3 , 150 MHz) δ 13.9, 50.7, 55.7, 62.3, 123.8, 148.2, 166.6. +APCI-MS calcd. for $\text{C}_7\text{H}_{12}\text{N}_3\text{O}_3$ $[\text{M} + \text{H}]^+$ 186.1, found 186.1.

5.3.1.3. Synthesis of ethyl 2-(4-(((methylsulfonyl)oxy)methyl)-1H-1,2,3-triazol-1-yl)acetate (13): [8a,b]. This compound is known compound [8a,b]. Compound **12** (100 mg, 0.54 mmol) was taken in a dry CH_2Cl_2 . Mesyl chloride (0.06 ml, 0.81 mmol) and triethyl amine (0.113 ml, 0.81 mmol) were added to the reaction mixture at 0 °C. The reaction mixture was stirred at 0 °C till the starting material was consumed. After that the reaction mixture was diluted with DCM and washed with water and dried over Na_2SO_4 and then evaporated in vacuum. The pure compound **13** was then isolated by column chromatography (si-gel, PE:EA = 2:1) as a colourless oil (129 mg, Yield 83%) and utilized immediately for the next step without further characterization.

5.3.1.4. Synthesis of ethyl 2-(4-(azidomethyl)-1H-1,2,3-triazol-1-yl)acetate (14): [8a,b]. This compound is known compound.^{8a–b} To a solution of the mesyl derivative **13** (129 mg, 0.523 mmol) in dry DMF (5 ml), NaN_3 (40.7 mg, 0.627 mmol) was added and stirred for 18 h at 50 °C. The reaction mixture was partitioned between EtOAc and water (20 ml each). The organic layer was washed with brine solution, dried with Na_2SO_4 , filtered and then evaporated. The title compound **14** was isolated by column chromatography (si-gel, PE:EA = 5:1) in pure form as white solid (98 mg, Yield 89%). mp 43–44 °C, IR (KBr) 3447, 3138, 3006, 2108, 1739, 1634, 1464, 1407, 1259, 1021, 771 cm^{-1} . ^1H NMR (CDCl_3 , 600 MHz) δ 1.29 (3H, t, $J = 6.6$ Hz), 4.27 (2H, q, $J = 7.2$ Hz), 4.51 (2H, s), 5.17 (2H, s), 7.17 (1H, s). $^{13}\text{C}\{1\text{H}\}$ NMR (CDCl_3 , 150 MHz) δ 14.0, 45.5, 50.9, 62.5, 124.0, 142.9, 166.2. +APCI-MS calcd. for $\text{C}_7\text{H}_{10}\text{N}_6\text{O}_2$ $[\text{M} + \text{H}]^+$ 211.1, found 211.1.

5.3.1.5. Synthesis of 2-(4-(azidomethyl)-1H-1,2,3-triazol-1-yl)acetic acid (15): [8a,b]. This compound is known compound.^{8a–b} To a solution of compound **14** in methanol, 2.5 (M) NaOH solution was added and stirred for about 2–3 h at room temperature until starting material was vanished. After that in the reaction mixture, dilute HCl was added until the pH became 4. Then it was partitioned between EtOAc and water (20 ml each). The organic layer was washed with brine solution, dried with Na_2SO_4 , filtered and then evaporated. The prepared title compound **15** was isolated as an amorphous white solid and used for next step without further purification (Yield 95%). IR (KBr) 3153, 2101, 1725, 1557, 1447, 1414, 1362, 1333, 1231, 1068, 822 cm^{-1} . ^1H NMR (CD_3OD , 400 MHz) δ 4.49 (2H, s), 5.30 (2H, s), 8.06 (1H, s). $^{13}\text{C}\{1\text{H}\}$ NMR (CD_3OD , 100 MHz) δ 46.1, 51.8, 126.6, 144.0, 169.9. –APCI-MS calcd. for $\text{C}_5\text{H}_5\text{N}_6\text{O}_2$ $[\text{M} - \text{H}]^-$ 181.1, found 181.2.

5.3.1.6. Synthesis of 2-(4-(aminomethyl)-1H-1,2,3-triazol-1-yl)acetic acid (16): [8a,b]. This compound is known compound.^{8a–b} To a solution of the compound **15** in methanol (200 mg, 1.1 mmol) Pd/C is added and to it hydrogen gas balloon was set and stir the reaction mixture for 3–4 h. The solvent methanol was then evaporated and the crude mass was dissolved in water and then filtered, filtrate is evaporated to afford the title compound **16** as a white solid with quantitative yield. mp 285–286 °C, IR (KBr) 3418, 3153, 1614, 1393, 1308, 1233 cm^{-1} . ^1H NMR (D_2O , 600 MHz) δ 4.34 (2H, s), 5.06 (2H, s), 8.07 (1H, s). $^{13}\text{C}\{1\text{H}\}$ NMR (D_2O , 150 MHz) δ 34.0, 53.2, 126.3, 139.6, 173.1. +APCI-MS calcd. for $\text{C}_5\text{H}_9\text{N}_4\text{O}_2$ $[\text{M} + \text{H}]^+$ 157.0727, found 157.0713.

5.3.1.7. Synthesis of $^{1/1\text{Al}}$ TAA (1): [8a,b]. This compound is known compound [8a,b]. In a solution of 2-(4-(azidomethyl)-1H-1,2,3-triazol-1-yl)acetic acid **16** (200 mg, 1.28 mmol) in 1:1 mixture of 1,4 dioxane and water (3 ml each) was added NaOH (102.6 mg, 2.56 mmol) followed by di-*t*-butyl dicarbonate (0.44 ml, 1.92 mmol) maintaining the pH between 7.5–8.5. The reaction mixture was stirred at room temperature for 20 h. The reaction mixture was washed with ethyl acetate (2 x 10 ml) and the aqueous phase was treated with dil. HCl to

bring pH 4 in cold condition. Immediately the solution was extracted with ethyl acetate and the organic layer was washed with water, brine, dried and evaporated under *vacuo* to furnish the Boc-protected 2-(4-(azidomethyl)-1H-1,2,3-triazol-1-yl)acetic acid **1** as white solid in pure form (265.4 mg, Yield 81%). mp 105–106 °C, ^1H NMR (CD_3OD , 400 MHz) δ 1.43 (9H, s), 4.31 (2H, s), 5.25 (2H, s), 7.87 (1H, s). $^{13}\text{C}\{1\text{H}\}$ NMR (CD_3OD , 100 MHz) δ 28.9, 36.8, 51.8, 80.6, 125.6, 147.4, 158.4, 170.0. –APCI-MS calcd. for $\text{C}_{10}\text{H}_{15}\text{N}_4\text{O}_4$ $[\text{M} - \text{H}]^-$ 255.2540, found 255.2255.

5.3.2. Synthesis of scaffold 2/1-scaffold (2)

The synthesis of 2/1-scaffold (**2**, $\text{BocNH}^{-2/1-\text{Al}}\text{TAA}$) was carried out following the **Scheme S1B** and followed the following steps.

5.3.2.1. Synthesis of methyl 2-(4-(2-hydroxyethyl)-1H-1,2,3-triazol-1-yl)acetate (19). Using general procedure of click reaction, we have obtained title compound **19** (1.577 g) from methyl azido acetate **17** as colourless oil (1.90 g) [prepared from methyl bromo acetate] and homopropargyl alcohol **18**. product yield = 83%. ^1H NMR (CDCl_3 , 400 MHz) δ 2.95 (2H, t, $J = 6.0$ Hz), 3.79 (3H, s), 3.92 (2H, bs), 5.14 (2H, s), 7.53 (1H, s). $^{13}\text{C}\{1\text{H}\}$ NMR (CDCl_3 , 100 MHz) δ 28.9, 50.8, 53.2, 61.6, 123.3, 146.1, 167.2. +APCI-MS calcd. for $\text{C}_7\text{H}_{12}\text{N}_3\text{O}_3$ $[\text{M} + \text{H}]^+$ 186.0873, found 186.0877.

Following the general procedure for the synthesis of mesylate from alcohol, we have obtained the title compound **20** (1.215 g) in 81% yield from the compound **19** (1.5 g). The mesylate was utilized for the next step without further purification or characterization.

Using general procedure for the synthesis of azide from mesylate, we have obtained the title azide **21** (1.032 g) from the mesylate **20** (1.2 g) as pale yellow gummy material in 86% yield. ^1H NMR (CDCl_3 , 400 MHz) δ 3.03 (2H, t, $J = 6.8$ Hz), 3.64 (2H, t, $J = 6.4$ Hz), 3.81 (3H, s), 5.17 (2H, s), 7.56 (1H, s). $^{13}\text{C}\{1\text{H}\}$ NMR (CDCl_3 , 100 MHz) δ 25.7, 50.6, 50.8, 53.1, 123.4, 144.8, 166.9. +APCI-MS calcd. for $\text{C}_7\text{H}_{11}\text{N}_6\text{O}_2$ $[\text{M} + \text{H}]^+$ 211.0938, found 211.0943

Using general procedure of methyl ester hydrolysis reaction, we have obtained the title compound **22** (0.94 g) from methyl 2-(4-(2-azidoethyl)-1H-1,2,3-triazol-1-yl)acetate (**21**, 1.0 g) as an amorphous white solid with yield of 94%. ^1H NMR (CD_3OD , 600 MHz) δ 3.02 (2H, t, $J = 7.2$ Hz), 3.63 (2H, t, $J = 6.4$ Hz), 5.16 (2H, s), 7.68 (1H, s). $^{13}\text{C}\{1\text{H}\}$ NMR (CDCl_3 , 150 MHz) δ 25.3, 50.3, 50.8, 123.7, 144.4, 168.2. +APCI-MS calcd. for $\text{C}_6\text{H}_7\text{N}_6\text{O}_2$ $[\text{M} + \text{H}]^+$ 195.0636, found 195.0633.

Using general procedure for the conversion of azide to amine, we have obtained free triazolyl amino acid scaffold **23** (0.855 g) from the azide **22** (0.9 g) as white solid with a yield of 95%. ^1H NMR (D_2O , 600 MHz) δ 3.13 (2H, t, $J = 6.6$ Hz), 3.35 (2H, t, $J = 6.6$ Hz), 5.04 (2H, s), 7.88 (1H, s). $^{13}\text{C}\{1\text{H}\}$ NMR (CDCl_3 , 100 MHz) δ 25.5, 41.7, 55.8, 127.9, 145.6, 175.9. Without further characterization the free amino acid was utilized for the next step.

5.3.2.2. Synthesis of scaffold 2/1-scaffold (2). Using general procedure for Boc protection, we have obtained title compound **2** (0.696 g) from amino acid **23** (0.8 g) as white solid with a yield of 87%. ^1H NMR (CDCl_3 , 400 MHz) δ 1.43 (9H, s), 2.91 (2H, t, $J = 6.4$ Hz), 3.40 (2H, q, $J = 8$ Hz, $J = 14$ Hz), 5.14 (2H, s), 7.60 (1H, s). $^{13}\text{C}\{1\text{H}\}$ NMR (CDCl_3 , 100 MHz) δ 29.8, 32.1, 43.6, 54.6, 83.4, 127.4, 149.4, 160.5, 172.2. $\text{C}_6\text{H}_7\text{N}_6\text{O}_2$ calcd. for $\text{C}_{11}\text{H}_{17}\text{N}_4\text{O}_4$ $[\text{M} + \text{H}]^+$ 269.1255, found 269.1251.

5.3.3. Synthesis of scaffold 1/2-scaffold (3)

The synthesis of 1/2-scaffold (**3**, $\text{BocNH}^{-2/1-\text{Al}}\text{TAA}$) was carried out following the **Scheme S2A** and followed the following steps.

5.3.3.1. Synthesis of methyl 3-azidopropanoate (25). Using general procedure for the conversion of bromo to azide, we have obtained the title compound **25** (1.96 g) from methyl 3-bromopropanoate **24** (2.0 g) as colourless oil. Product yield = 98%. IR (KBr) 2956, 2104, 1743

cm^{-1} . The azide was used for the next step without further purification and characterization.

5.3.3.2. Synthesis of methyl 3-(4-(hydroxymethyl)-1H-1,2,3-triazol-1-yl)propanoate (26). Using general procedure for click reaction, we have obtained the title compound **26** (1.539 g) from methyl 3-azidopropanoate (**25**, 1.90 g) as white solid. Yield = 81%. ^1H NMR (CDCl_3 , 400 MHz) δ 2.91 (2H, t, $J = 6.4$ Hz), 3.63 (3H, s), 4.36–4.37 (1H, d), 4.58 (2H, t, $J = 6.4$ Hz), 4.67–4.68 (2H, d, $J = 5.6$ Hz), 7.63 (1H, s). $^{13}\text{C}\{1\text{H}\}$ NMR (CDCl_3 , 100 MHz) δ 34.1, 45.4, 51.9, 55.5, 122.8, 147.7, 170.9. + APCI MS calcd. for $\text{C}_7\text{H}_{12}\text{N}_3\text{O}_3$ $[\text{M}+\text{H}]^+$ 186.0873, found 186.0872.

5.3.3.3. Synthesis of methyl 3-(4-((methylsulfonyl)oxy)methyl)-1H-1,2,3-triazol-1-yl)propanoate (27). Using general procedure for the conversion of alcohol to mesylate derivative, we have obtained the title compound **27** (1.215 g) from compound **26** (1.5 g) as yellow gummy material. Yield = 81%. The mesylate was used for the next step without further purification and characterization.

5.3.3.4. Synthesis of methyl 3-(4-(azidomethyl)-1H-1,2,3-triazol-1-yl)propanoate (28). Using general procedure for the conversion of mesylate to azide derivative, we have obtained the title compound **28** (1.02 g) from compound mesylate **27** (1.2 g) as white solid. Yield = 85%. ^1H NMR (CDCl_3 , 400 MHz) δ 2.899 (2H, t, $J = 6.0$ Hz), 3.59 (3H, s), 4.37 (2H, s), 4.58 (2H, t, $J = 6.4$ Hz), 7.66 (1H, s). $^{13}\text{C}\{1\text{H}\}$ NMR (CDCl_3 , 100 MHz) δ 34.2, 45.4, 45.6, 52.1, 123.4, 142.2, 170.9. + APCI MS calcd. for $\text{C}_7\text{H}_{11}\text{N}_6\text{O}_2$ $[\text{M}+\text{H}]^+$ 211.0938, found 211.0938.

5.3.3.5. Synthesis of 3-(4-(azidomethyl)-1H-1,2,3-triazol-1-yl)propanoic acid (29). Using general procedure for methyl ester hydrolysis, we have obtained the title compound **29** (0.93 g) from methyl 3-(4-(azidomethyl)-1H-1,2,3-triazol-1-yl)propanoate, **28** (1.0 g) as white solid. Yield = 93%. ^1H NMR (CDCl_3 , 400 MHz) δ 2.99 (2H, t, $J = 6.4$ Hz), 4.47 (2H, s), 4.69 (2H, t, $J = 6.4$ Hz), 7.95 (1H, s). $^{13}\text{C}\{1\text{H}\}$ NMR (CDCl_3 , 100 MHz) δ 35.2, 47.3, 48.6, 125.6, 143.9, 173.9. + APCI MS calcd. for $\text{C}_6\text{H}_7\text{N}_6\text{O}_2$ $[\text{M}+\text{H}]^-$ 195.0636, found 195.0618.

5.3.3.6. Synthesis of 3-(4-(aminomethyl)-1H-1,2,3-triazol-1-yl)propanoic acid (30). Using general procedure for the conversion of azide to amine, we have obtained the title compound **30** (0.855 g) from azido acid **29** (0.9 g) as white solid. Yield = 95%. ^1H NMR (CDCl_3 , 600 MHz) δ 2.81 (2H, t, $J = 6.6$ Hz), 4.33 (2H, s), 4.67 (2H, t, $J = 6.6$ Hz), 8.08 (1H, s). $^{13}\text{C}\{1\text{H}\}$ NMR (CDCl_3 , 150 MHz) δ 33.9, 37.4, 47.7, 125.1, 139.4, 178.4. The acid was used for the next step without further purification and characterization.

5.3.3.7. Synthesis of $^{2/1}\text{AlTAA}$ (3). Using general procedure for Boc protection, we have obtained the title compound **3** (0.608 g) from 3-(4-(aminomethyl)-1H-1,2,3-triazol-1-yl)propanoic acid (**30**, 0.80 g) as white solid. Yield = 76%. ^1H NMR (CDCl_3 , 600 MHz) δ 1.40 (9H, s), 2.96 (2H, t, $J = 6.6$ Hz), 4.34 (2H, d, $J = 5.4$ Hz), 4.67 (2H, t, $J = 5.4$ Hz), 7.69 (1H, s). $^{13}\text{C}\{1\text{H}\}$ NMR (CDCl_3 , 150 MHz) δ 28.4, 34.6, 35.8, 46.0, 80.2, 123.4, 145.3, 156.4, 173.4. + APCI MS calcd. for $\text{C}_{11}\text{H}_{17}\text{N}_4\text{O}_4$ $[\text{M}+\text{H}]^+$ 269.1255, found 269.1247.

5.3.4. Synthesis of scaffold 2/2-scaffold (4)

The synthesis of 2/2-scaffold (**4**, $\text{BocNH-}^{2/2}\text{-AlTAA}$) was carried out following the **Scheme S2B** and followed the following steps.

5.3.4.1. Synthesis of methyl 3-(4-(2-hydroxyethyl)-1H-1,2,3-triazol-1-yl)propanoate (31). Using general procedure for click reaction, we have obtained the title compound **31** (1.501 g) as white solid from methyl 3-azidopropanoate **25** (1.90 g) and the homopropargyl alcohol **18**.

Product yield = 79%. ^1H NMR (CDCl_3 , 400 MHz) δ 2.86–2.93 (4H, m), 3.19–3.28 (1H, bs), 3.66 (3H, s), 3.86–3.87 (2H, bd, $J = 4$ Hz), 4.55–4.60 (2H, q, $J = 6.0$ Hz, 11.2 Hz), 7.47 (1H, s). $^{13}\text{C}\{1\text{H}\}$ NMR (CDCl_3 , 100 MHz) δ 28.8, 34.5, 45.5, 52.3, 61.5, 122.6, 145.5, 171.2. + APCI MS calcd. for $\text{C}_8\text{H}_{14}\text{N}_3\text{O}_3$ $[\text{M}+\text{H}]^+$ 200.1029, found 200.1031.

5.3.4.2. Synthesis of methyl 3-(4-(2-((methylsulfonyl)oxy)ethyl)-1H-1,2,3-triazol-1-yl)propanoate (32). Using general procedure for the conversion of alcohol to mesylate, we have obtained the title compound **32** (1.19 g) as colourless gummy material from methyl 3-(4-(2-hydroxyethyl)-1H-1,2,3-triazol-1-yl)propanoate (**31**, 1.4 g). Product yield = 85%. The mesylate was used for the next step without further purification and characterization.

5.3.4.3. Synthesis of methyl 3-(4-(2-azidoethyl)-1H-1,2,3-triazol-1-yl)propanoate (33). Using general procedure for the conversion of mesylate to azide derivative, we have obtained the title compound **33** (0.902 g) from methyl 3-(4-(2-((methylsulfonyl)oxy)ethyl)-1H-1,2,3-triazol-1-yl)propanoate (**32**, 1.1 g) as colourless gummy material. Product yield = 82%. ^1H NMR (CDCl_3 , 400 MHz) δ 2.87–2.91 (4H, m), 3.52 (2H, t, $J = 7.2$ Hz), 3.66 (3H, s), 4.55 (2H, t, $J = 6.8$ Hz), 7.47 (1H, s). $^{13}\text{C}\{1\text{H}\}$ NMR (CDCl_3 , 100 MHz) δ 25.6, 34.4, 45.4, 50.5, 52.1, 122.6, 144.0, 170.9. + APCI MS calcd. for $\text{C}_8\text{H}_{13}\text{N}_6\text{O}_2$ $[\text{M}+\text{H}]^+$ 225.1094, found 225.1096.

5.3.4.4. Synthesis of 3-(4-(2-azidoethyl)-1H-1,2,3-triazol-1-yl)propanoic acid (34). Using general procedure for the methyl ester hydrolysis, we have obtained the title compound **34** (0.752 g) from methyl 3-(4-(2-azidoethyl)-1H-1,2,3-triazol-1-yl)propanoate (**33**, 0.8 g) as white solid. Product yield = 94%. ^1H NMR (CDCl_3 , 400 MHz) δ 2.95–3.02 (4H, m), 3.57 (2H, t, $J = 6.4$ Hz), 4.62 (2H, t, $J = 6.8$ Hz), 7.55 (1H, s). $^{13}\text{C}\{1\text{H}\}$ NMR (CDCl_3 , 100 MHz) δ 25.6, 34.6, 45.8, 52.1, 123.3, 144.2, 174.2. + APCI MS calcd. for $\text{C}_7\text{H}_9\text{N}_6\text{O}_2$ $[\text{M}-\text{H}]^-$ 209.0792, found 209.0801.

5.3.4.5. Synthesis of 3-(4-(2-aminoethyl)-1H-1,2,3-triazol-1-yl)propanoic acid (35). Using general procedure for the conversion of azide to amine, we have obtained the title compound **35** (0.644 g) from 3-(4-(2-azidoethyl)-1H-1,2,3-triazol-1-yl)propanoic acid (**34**, 0.7 g) as white solid. Product yield = 92%. ^1H NMR (D_2O , 400 MHz) δ 2.79 (4H, m), 3.11 (2H, t, $J = 6.8$ Hz), 3.34 (2H, t, $J = 7.2$ Hz), 7.88 (1H, s). $^{13}\text{C}\{1\text{H}\}$ NMR (CDCl_3 , 100 MHz) δ 22.9, 37.6, 47.7, 57.9, 124.1, 142.9, 178.6. The acid was used for the next step without further purification and characterization.

5.3.4.6. Synthesis of $^{2/2}\text{AlTAA}$ (4). Using general procedure for Boc protection, we have obtained the title compound **4** (0.474 g) from 3-(4-(2-aminoethyl)-1H-1,2,3-triazol-1-yl)propanoic acid (**35**, 0.6 g) as white solid. Product yield = 79%. ^1H NMR (CDCl_3 , 600 MHz) δ 1.41 (9H, s), 2.88 (2H, t, $J = 6.5$ Hz), 2.98 (2H, t, $J = 5.8$ Hz), 3.42 (2H, s), 4.63 (2H, t, $J = 6.3$ Hz), 5.14 (1H, s), 7.53 (1H, s). $^{13}\text{C}\{1\text{H}\}$ NMR (CDCl_3 , 150 MHz) δ 26.2, 28.6, 34.7, 40.1, 45.9, 79.8, 122.9, 145.4, 156.5, 173.4. -APCI MS calcd. for $\text{C}_{11}\text{H}_{17}\text{N}_4\text{O}_4$ $[\text{M}-\text{H}]^-$ 269.1255, found 269.1261.

5.3.5. Synthesis of the peptides (5–8)

Peptides **5–6** were synthesized following **Scheme 3A-B** and peptides **7–8** were synthesized following **Scheme 4A-B**.

5.3.5.1. Synthesis of BocNH-Leu- $^{TPy}\text{Ala}^{\text{Do}}$ -CONMe(OMe) (38). This compound is known compound. $^{8a-b}$ Using the general procedure of [3 + 2]cyclo-addition reaction, starting from 200 mg (0.52 mmol) of azide derivative of dipeptide **36** $^{8a-b}$ and 140 mg (0.62 mmol) of 1-ethynyl pyrene **37**, 247 mg (0.40 mmol) of the title compound **38** was isolated as a light brown solid material (Si-gel, PE : EtOAc = 1:1). Yield

78%, IR (KBr) 3450, 2958, 2928, 2102, 1653, 1509, 1390, 1167, 1049, 848 cm^{-1} . ^1H NMR (CDCl_3 , 600 MHz), δ 0.89 (6H, d, $J = 5.4$ Hz), 1.38 (9H, s), 1.52–1.48 (1H, m), 1.67–1.59 (2H, m), 3.29 (3H, s), 3.7 (3H, s), 4.11 (1H, bs), 4.89 (1H, dd, $J = 4.2$ Hz, 9.6 Hz), 4.95 (1H, d, $J = 6.6$ Hz), 5.05 (1H, bs), 5.36 (1H, bs), 7.22 (1H, d, $J = 5.4$ Hz), 7.99 (1H, t, $J = 7.2$ Hz), 8.06 (2H, d, $J = 4.8$ Hz), 8.09 (1H, t, $J = 9.0$ Hz), 8.18–8.15 (3H, m), 8.30 (1H, s), 8.31 (1H, s), 8.79 (1H, d, $J = 9.0$ Hz). $^{13}\text{C}\{1\text{H}\}$ NMR (CDCl_3 , 150 MHz), δ 21.9, 23.1, 24.9, 28.4, 32.9, 41.1, 50.4, 50.7, 53.9, 62.1, 80.4, 124.8, 124.9, 125.0, 150.2, 125.3, 125.4, 126.1, 127.4, 127.5, 127.8, 128.2, 128.7, 131.1, 131.4, 131.5, 147.8, 155.9, 168.2, 173.2. + APCI MS calcd for $\text{C}_{34}\text{H}_{41}\text{N}_6\text{O}_5$ $[\text{M} + \text{H}]^+$ 613.3133, found 613.3132.

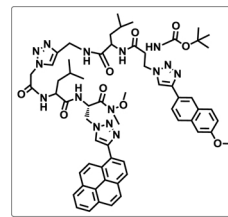
5.3.5.2. Synthesis of TFA salt of BocNH–Leu–^{TPy}Ala^{Do}–CONMe(OMe) (39). Using the general procedure of Boc-deprotection, the compound **38** (240 mg, 0.40 mmol) was deprotected and the product **39** was obtained in quantitative yield as light brown solid and were used without further purification and characterization.

5.3.5.3. Synthesis of BocNH–^{1/1Al}TAA–Leu–^{TPy}Ala^{Do}–CONMe(OMe) (40). To a solution of *N*-protected aliphatic amino acid scaffold (**1**, 160 mg, 0.625 mmol) in dry DMF, (EDC.HCl) (178 mg, 0.937 mmol), followed by DMAP (288 mg, 1.87 mmol) were added at 0 °C. Next, the amine salt of Weinreb amide, the dipeptide **39** (390 mg, 0.625 mmol) was added and the reaction mixture was stirred for 30 min at 0 °C and then 18 h at room temperature. After completion of the reaction (monitored by TLC) the work up was done with EtOAc and water. The organic layer was washed with brine solution. The product tripeptide **40** (342 mg, 0.456 mmol) was isolated in pure form by column chromatography (Si-gel, EtOAc) as light brown solid compound. Yield 73%. ^1H NMR (CDCl_3 , 600 MHz) δ 0.81–0.91 (6H, m), 1.37 (9H, s), 1.49–1.63 (3H, m), 3.27 (3H, s), 3.80 (3H, s), 4.22 (2H, s), 4.44–4.53 (1H, m), 4.87 (2H, s), 4.97 (1H, d, $J = 8.1$ Hz), 5.01–5.07 (1H, m), 5.08–5.14 (1H, m), 5.20 (1H, s), 5.41 (1H, d, $J = 6.3$ Hz), 7.51 (1H, bs), 7.56 (1H, s), 8.00–8.10 (m, 5H), 8.14–8.23 (4H, m), 8.64 (1H, d, $J = 8.9$ Hz). $^{13}\text{C}\{1\text{H}\}$ NMR (CDCl_3 , 100 MHz) δ 21.9, 22.9, 24.9, 29.9, 32.8, 36.3, 40.2, 40.3, 43.4, 50.5, 51.9, 52.5, 52.6, 52.7, 54.8, 61.9, 62.1, 62.3, 79.7, 113.9, 113.9, 116.3, 116.8, 123.1, 123.9, 123.9, 124.0, 124.2, 124.6, 124.7, 124.8, 124.9, 125.0, 125.1, 125.3, 125.4, 125.6, 125.7, 125.8, 125.8, 126.3, 126.4, 127.3, 127.5, 128.1, 128.4, 128.5, 128.5, 128.6, 128.7, 128.9, 131.0, 131.4, 131.5, 131.9, 135.0, 135.1, 142.0, 142.3, 147.6, 151.9, 155.9, 161.4, 166.1, 171.9. + APCI MS calcd. for $\text{C}_{39}\text{H}_{47}\text{N}_{10}\text{O}_6$ $[\text{M} + \text{H}]^+$ 751.3675, found 751.3675.

5.3.5.4. Synthesis of TFA salt of BocNH–^{1/1Al}TAA–Leu–^{TPy}Ala^{Do}–CONMe(OMe) (41). Using the general procedure of Boc-deprotection, compound **40** (300 mg, 0.4 mmol) was reacted with TFA to get the product **41** in quantitative (95%) yield as brown solid material and was used for the next step without further purification and characterization.

5.3.5.5. Synthesis of BocNH–^{TMnap}Ala^{Do}–Leu–^{1/1Al}TAA–Leu–^{TPy}Ala^{Do}–CONMe(OMe) (5). Using general procedure of peptide coupling, the acid compound **42** (200 mg, 0.38 mmol)^{8a,b} was taken as starting material and amine compound **41** (290 mg, 0.38 mmol) was reacted with it. After completion of reaction, 162 mg (0.141 mmol) of the title compound **5** was isolated in pure form by column chromatography (Si-gel, PE : EtOAc = 1:4) as light brown solid material. Yield 37%. IR (KBr) 3423, 3310, 2925, 2106, 1673, 1557, 1456, 1432, 1163, 1027, 849 cm^{-1} . ^1H NMR (CDCl_3 , 600 MHz) δ 0.48–0.72 (12H, m), 1.20 (9H, s), 1.53–1.61 (6H, m), 3.14 (3H, s), 3.31 (3H, s), 3.86 (3H, s), 4.30 (4H, dd, $J = 26.2$, 11.2 Hz), 4.48–4.58 (2H, m), 4.75 (2H, dd, $J = 13.9$, 3.8 Hz), 4.83 (2H, d, $J = 9.2$ Hz), 4.97–5.04 (1H, m), 5.07–5.16 (2H, m), 7.85 (2H, d, $J = 8.6$ Hz), 8.05–8.13 (2H, m), 8.23 (5H, ddd, $J = 15.8$, 8.8, 4.8 Hz), 8.27–8.38 (7H, m), 8.47 (2H, s), 8.52 (1H, s), 8.70 (1H, s), 8.79 (2H, t, $J = 9.2$ Hz). $^{13}\text{C}\{1\text{H}\}$ NMR (CDCl_3 , 150 MHz)

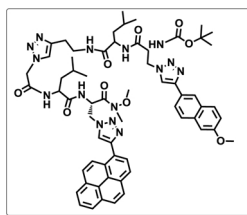
δ 21.4, 21.7, 22.1, 22.7, 22.9, 23.1, 23.2, 24.1, 24.2, 24.3, 28.0, 29.0, 43.4, 45.9, 49.5, 49.7, 51.4, 51.5, 51.7, 55.0, 55.3, 79.2, 123.3, 123.3, 123.9, 124.3, 125.0, 125.1, 125.4, 125.9, 126.3, 126.5, 126.8, 127.4, 127.5, 127.5, 127.6, 127.8, 127.9, 128.0, 128.7, 129.6, 130.4, 130.6, 130.6, 130.9, 132.1, 133.2, 133.9, 141.3, 141.4, 145.8, 146.0, 155.1, 165.4, 167.7, 168.8, 175.3, 177.2. + APCI MS calcd. for $\text{C}_{61}\text{H}_{72}\text{N}_{15}\text{O}_9$ $[\text{M} + \text{H}]^+$ 1158.5632, found 1158.5646.



5.3.5.6. Synthesis of BocNH–^{1/2Al}TAA–Leu–^{TPy}Ala^{Do}–CONMe(OMe) (43). Following the similar procedure of DMAP mediated peptide coupling reaction, we have obtained tripeptide **43** from *N*-protected aliphatic amino acid scaffold **2** (160 mg, 0.625 mmol) as light brown solid compound. Yield 71%. ^1H NMR (CDCl_3 , 600 MHz) δ 0.82–0.91 (6H, m), 1.37 (9H, s), 1.49–1.63 (3H, m), 2.59 (1H, s), 2.87 (1H, s), 3.28 (3H, s), 3.33–3.43 (3H, m), 3.50–3.61 (1H, m), 3.81 (3H, s), 4.42–4.50 (1H, m), 4.52–4.62 (1H, m), 4.88 (1H, s), 4.98 (2H, s), 5.04 (1H, m), 5.09–5.18 (1H, m), 5.42 (1H, s), 7.04 (3H, bs), 7.55 (2H, s), 7.97–8.12 (5H, m), 8.15–8.24 (4H, m), 8.64 (1H, d, $J = 9.2$ Hz). $^{13}\text{C}\{1\text{H}\}$ NMR (CDCl_3 , 150 MHz) δ 21.9, 22.9, 23.0, 24.9, 24.9, 26.2, 26.4, 28.6, 32.5, 32.8, 39.7, 40.1, 41.0, 49.8, 50.5, 51.9, 52.5, 52.8, 61.9, 62.2, 66.0, 79.3, 123.5, 123.6, 124.7, 124.7, 124.8, 124.9, 125.0, 125.1, 125.3, 125.4, 125.7, 125.8, 126.4, 126.5, 127.4, 127.5, 128.1, 128.5, 128.7, 129.9, 131.0, 131.5, 147.5, 151.6, 155.9, 165.8, 166.2, 171.8. + APCI MS calcd. for $\text{C}_{40}\text{H}_{49}\text{N}_{10}\text{O}_6$ $[\text{M} + \text{H}]^+$ 765.3831, found 765.3839.

5.3.5.7. Synthesis of TFA salt of BocNH–^{1/2Al}TAA–Leu–^{TPy}Ala^{Do}–CONMe(OMe) (44). Using the general procedure of Boc-deprotection, compound **43** (300 mg, 0.39 mmol) was reacted with TFA to get the product **44** as brown solid material in quantitative (96%) yield and was used for the next step without further purification and characterization.

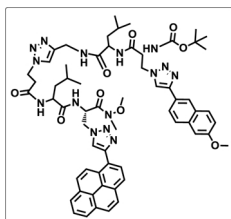
5.3.5.8. Synthesis of BocNH–^{TMnap}Ala^{Do}–Leu–^{1/2Al}TAA–Leu–^{TPy}Ala^{Do}–CONMe(OMe) (6). Using general procedure of peptide coupling reaction, the acid compound **42** (200 mg, 0.38 mmol) was taken as a starting material then (296 mg, 0.38 mmol) of amine compound **44** was reacted with it. After completion of reaction 151 mg (0.129 mmol) of the title compound **6** was isolated in pure form by column chromatography (Si-gel, PE : EtOAc = 1:4) as light brown solid material. Yield 34%. IR (KBr) 3308, 2924, 2105, 1680, 1657, 1549, 1465, 1246, 1163, 1024, 849 cm^{-1} . ^1H NMR (CDCl_3 , 600 MHz) δ 0.82–0.91 (12H, m), 1.29 (9H, s), 1.39–1.51 (6H, m), 3.16 (3H, s), 3.41 (3H, s), 3.74 (2H, d, $J = 22.0$ Hz), 3.87 (3H, s), 4.37 (2H, s), 4.53 (1H, s), 4.55–4.63 (1H, m), 4.72–4.79 (2H, m), 4.85 (2H, d, $J = 13.3$ Hz), 4.98 (1H, s), 5.03 (1H, d, $J = 3.4$ Hz), 5.09 (2H, d, $J = 8.8$ Hz), 5.37 (1H, s), 7.18 (1H, d, $J = 7.9$ Hz), 7.83–7.92 (2H, m), 8.07–8.14 (2H, m), 8.24 (5H, dd, $J = 7.9$, 5.4 Hz), 8.30–8.36 (6H, m), 8.39 (1H, d, $J = 7.9$ Hz), 8.44 (1H, s), 8.48 (1H, s), 8.53 (1H, s), 8.68 (1H, s), 8.82 (1H, d, $J = 9.3$ Hz). $^{13}\text{C}\{1\text{H}\}$ NMR (CDCl_3 , 150 MHz) δ 21.5, 21.6, 21.7, 22.7, 22.9, 23.1, 23.1, 23.2, 24.1, 28.0, 28.1, 49.4, 49.8, 51.4, 51.7, 52.4, 55.1, 55.5, 78.4, 123.9, 124.3, 124.4, 124.9, 125.2, 126.3, 126.5, 126.6, 126.7, 127.0, 127.1, 127.4, 127.6, 127.7, 127.8, 127.9, 128.0, 128.1, 128.3, 128.5, 130.4, 130.6, 130.7, 130.7, 130.9, 131.1, 133.3, 145.8, 146.0, 148.8, 149.4, 154.8, 165.2, 167.8, 170.9, 172.0. + APCI MS calcd. for $\text{C}_{62}\text{H}_{74}\text{N}_{15}\text{O}_9$ $[\text{M} + \text{H}]^+$ 1172.5788, found 1172.5771.



5.3.5.9. Synthesis of BocNH-^{2/1Al}TAA-Leu-^{TPy}Ala^{Do}-CONMe(OMe) (45). Following the similar procedure of DMAP mediated peptide coupling we have obtained tripeptide **45** from *N*-protected aliphatic amino acid scaffold **3** (160 mg, 0.625 mmol) as yellowish brown gummy compound. Yield 67%. ¹H NMR (CDCl₃, 600 MHz) δ 0.84–0.94 (6H, m), 1.25 (9H, s), 1.50 (2H, m), 1.59–1.65 (1H, m), 2.69 (2H, s), 3.31 (3H, s), 3.86 (3H, s), 4.31–4.44 (1H, m), 4.48–4.66 (2H, m), 4.74–4.85 (5H, m), 4.94 (2H, dd, *J* = 19.7, 9.6 Hz), 5.07 (1H, s), 5.40 (1H, d, *J* = 2.0 Hz), 5.56 (6H, s), 5.99 (1H, dd, *J* = 26.0, 7.3 Hz), 6.35 (6H, d, *J* = 23.5 Hz), 7.32 (1H, d, *J* = 8.8 Hz), 7.98–8.13 (5H, m), 8.17–8.28 (4H, m), 8.72 (3H, d, *J* = 9.3 Hz). + APCI MS calcd. for C₄₀H₄₉N₁₀O₆ [M + H]⁺ 765.3831, found 765.3826.

5.3.5.10. Synthesis of TFA salt of BocNH-^{2/1Al}TAA-Leu-^{TPy}Ala^{Do}-CONMe(OMe) (46). Using the general procedure of Boc-deprotection, compound **45** (300 mg, 0.39 mmol) was reacted with TFA to get the product **46** in quantitative (95%) yield and was used for the next step without further purification and characterization.

5.3.5.11. Synthesis of BocNH-^{TMnap}Ala^{Do}-Leu-^{2/1Al}TAA-Leu-^{TPy}Ala^{Do}-CONMe(OMe) (7). Using general procedure of peptide coupling, the acid compound **42** (200 mg, 0.38 mmol) was taken as a starting material then (296 mg, 0.38 mmol) of amine compound **45** was reacted with it. After completion of reaction 138 mg (0.118 mmol) of the title compound **7** was isolated in pure form by column chromatography (Sigel, PE : EtOAc = 1:4) as light brown solid material. Yield 31%. IR (KBr) 3299, 2957, 2106, 1683, 1660, 1541, 1389, 1163, 1056, 848 cm⁻¹. ¹H NMR (CDCl₃, 600 MHz) δ 0.82–0.87 (12H, m), 1.68 (9H, s), 1.80–1.87 (6H, m), 3.17 (3H, s), 3.41 (3H, s), 3.76 (4H, s), 3.90 (2H, d, *J* = 9.3 Hz), 4.32 (3H, m), 4.68 (1H, dd, *J* = 13.7, 7.5 Hz), 4.76 (2H, m), 4.78–4.93 (3H, m), 5.34 (2H, bs), 5.51 (1H, bs), 7.50 (1H, d, *J* = 7.9 Hz), 8.02–8.06 (1H, m), 8.13 (3H, dt, *J* = 14.9, 7.8 Hz), 8.24–8.29 (6H, m), 8.33–8.39 (7H, m), 8.41 (1H, d, *J* = 7.9 Hz), 8.52 (1H, bs), 8.74 (1H, s), 8.85 (1H, d, *J* = 9.3 Hz). ¹³C{¹H} NMR (CDCl₃, 150 MHz) δ 22.0, 22.1, 23.0, 23.5, 23.7, 24.7, 24.8, 25.2, 25.3, 28.0, 29.6, 29.7, 32.8, 50.1, 50.4, 51.5, 51.7, 51.9, 53.5, 53.7, 59.5, 62.2, 79.8, 124.4, 124.6, 124.9, 125.3, 125.7, 125.8, 125.9, 126.2, 126.3, 126.6, 127.1, 127.3, 127.7, 127.9, 128.0, 128.2, 128.3, 128.4, 128.6, 128.9, 128.9, 130.3, 131.0, 131.2, 131.4, 131.6, 141.5, 146.5, 150.7, 157.5, 169.9, 169.9, 172.3, 173.1, 173.3. + APCI MS calcd. for C₆₂H₇₄N₁₅O₉ [M + H]⁺ 1172.5788, found 1172.5719.

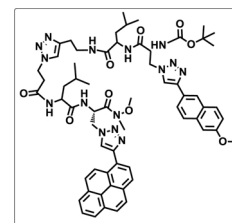


5.3.5.12. Synthesis of BocNH-^{2/2Al}TAA-Leu-^{TPy}Ala^{Do}-CONMe(OMe) (47). Following the similar procedure of DMAP mediated peptide coupling we have obtained tripeptide **47** from *N*-protected aliphatic amino acid scaffold **4** (160 mg, 0.625 mmol) as yellowish brown gummy

compound. Yield 65%. ¹H NMR (CDCl₃, 600 MHz) δ 0.79–0.92 (6H, m), 1.38 (9H, s), 1.48–1.66 (3H, m), 2.31 (2H, d, *J* = 15.7 Hz), 2.68 (1H, dt, *J* = 31.1, 12.2 Hz), 2.92–2.74 (1H, m), 3.20 (1H, s), 3.26 (3H, s), 3.50–3.64 (1H, m), 3.72 (1H, d, *J* = 1.5 Hz), 3.80 (3H, s), 4.20 (2H, d, *J* = 5.5 Hz), 4.33 (1H, dd, *J* = 15.2, 7.6 Hz), 4.42 (1H, s), 4.57 (1H, dd, *J* = 8.3, 4.2 Hz), 4.88 (2H, s), 5.42 (1H, d, *J* = 5.2 Hz), 7.04 (1H, d, *J* = 20.9 Hz), 7.22 (1H, s), 7.49 (1H, s), 7.93–8.09 (5H, m), 8.11–8.20 (4H, m), 8.67 (1H, dd, *J* = 24.4, 9.0 Hz). ¹³C{¹H} NMR (CDCl₃, 150 MHz) δ 21.8, 22.0, 23.0, 23.1, 24.8, 24.9, 28.6, 29.9, 32.8, 40.4, 41.5, 46.0, 50.6, 51.9, 52.3, 62.2, 66.0, 79.7, 124.7, 124.8, 124.9, 125.0, 125.1, 125.3, 125.5, 125.6, 126.2, 126.3, 127.4, 127.5, 127.9, 128.0, 128.3, 128.4, 128.7, 130.9, 131.0, 131.4, 131.4, 131.5, 131.5, 131.5, 132.1, 145.2, 147.5, 155.9, 168.4, 169.9, 172.6. + APCI MS calcd. for C₄₁H₅₁N₁₀O₆ [M + H]⁺ 779.3988, found 779.3991.

5.3.5.13. Synthesis of TFA salt of BocNH-^{2/2Al}TAA-Leu-^{TPy}Ala^{Do}-CONMe(OMe) (48). Using the general procedure of Boc-deprotection, compound **47** (300 mg, 0.39 mmol) was reacted with TFA to get the product **48** in quantitative (96%) yield and was used for the next step without further purification and characterization.

5.3.5.14. Synthesis of BocNH-^{TMnap}Ala^{Do}-Leu-^{2/2Al}TAA-Leu-^{TPy}Ala^{Do}-CONMe(OMe) (8). Using general procedure of peptide coupling, the acid compound **42** (200 mg, 0.38 mmol) was taken as starting material then (301 mg, 0.37 mmol) of amine compound **48** was reacted with it. After completion of reaction 166 mg (0.14 mmol) of the title compound **8** was isolated in pure form by column chromatography (Sigel, PE : EtOAc = 1:4) as light brown amorphous solid material. Yield 37%. IR (KBr) 3296, 2924, 2105, 1648, 1546, 1435, 1171, 1053, 849 cm⁻¹. ¹H NMR (CDCl₃, 600 MHz) δ 0.67–0.71 (6H, m), 0.83 (6H, m), 1.25–1.36 (3H, m), 1.39–1.51 (3H, m), 1.73 (9H, s), 3.12 (3H, d, *J* = 18 Hz), 3.15 (3H, s), 3.47–3.53 (1H, m), 3.70 (2H, s), 3.75 (5H, s), 4.19–4.35 (4H, m), 4.66 (1H, dd, *J* = 13.8, 7.4 Hz), 4.74 (2H, dd, *J* = 13.9, 8.3 Hz), 4.83 (3H, dt, *J* = 21.1, 7.7 Hz), 5.32 (2H, s), 5.49 (1H, s), 7.99–8.04 (1H, m), 8.10 (3H, dt, *J* = 11.4, 7.6 Hz), 8.16–8.27 (6H, m), 8.27–8.36 (8H, m), 8.39 (1H, d, *J* = 7.9 Hz), 8.48 (1H, bs), 8.71 (2H, s), 8.82 (1H, d, *J* = 9.3 Hz). ¹³C{¹H} NMR (CDCl₃, 150 MHz) δ 20.3, 22.0, 22.1, 22.2, 23.0, 23.1, 23.5, 23.7, 24.7, 24.8, 25.5, 32.7, 39.3, 39.7, 39.9, 40.0, 40.1, 40.3, 40.4, 40.6, 40.7, 41.2, 41.5, 49.3, 50.1, 50.4, 51.3, 51.5, 51.9, 58.7, 62.1, 63.7, 65.6, 87.5, 124.4, 124.4, 124.6, 124.7, 124.9, 125.0, 125.3, 125.5, 125.7, 125.8, 125.9, 126.1, 126.1, 126.2, 126.5, 127.1, 127.4, 127.7, 127.8, 128.0, 128.1, 128.2, 128.3, 128.5, 128.6, 129.2, 131.0, 131.1, 131.2, 131.3, 131.6, 146.6, 154.5, 169.9, 171.3, 173.1, 173.2, 173.3. + APCI MS calcd. for C₆₃H₇₆N₁₅O₉ [M + H]⁺ 1186.5945, found 1186.5976.



5.4. Photophysical studies of the synthesized peptides: general procedures

5.4.1. UV-vis measurements

The UV-visible spectra of all final peptides and UNNAs (10 μM) were measured in different solvents using a UV-vis spectrophotometer (SHIMADZU, UV-2550) with a cell of 1 cm path length. The measurements were done in absorbance mode. The sample solutions absorbance values were measured in the wavelength range of 200–700 nm. All the sample solutions were prepared freshly just before doing the experiment.

5.4.2. Fluorescence experiments

All the sample solutions for fluorescence measurements (**HORIBA Scientific, Fluoromax-4**) were also prepared freshly just before doing the experiment. Fluorescence spectra were obtained using a fluorescence spectrophotometer at 25 °C using 1 cm path length cell. The wavelengths for excitation in all the cases were set at the absorption maxima of each sample in each solvent. The emission spectra were measured in the wavelength regime of 300–700 nm with an integration time of 0.2 s. From 2.0 ml 500 μM stock solution, 2 ml of 10 μM concentration of solution was used for fluorescence experiment in 1 ml cell. Fluorescence emissions were recorded by exciting the sample solutions at their absorption maxima. Steady-state fluorescence emission spectra were recorded at room temperature as an average of five scans using an excitation slit of 3.0 nm, emission slit 3.0 nm, and scan speed of 120 nm/min. Using quinine sulphate as a reference, the fluorescence quantum yields (Φ_f) were determined with the known Φ_f (0.55) in 0.1 M solution in sulphuric acid. Following equation was used to calculate the quantum yield,

$$\Phi_S = \Phi_R \frac{F_S^{Area} Abs_R n_S^2}{F_R^{Area} Abs_S n_R^2}$$

where, Φ_R is the quantum yield of standard reference, F_S^{Area} (sample) and F_R^{Area} (reference) are the integrated emission peak areas, Abs_S (sample) and Abs_R (reference) are the absorbances at the excitation wavelength, and n_S (sample) and n_R (reference) are the refractive indices of the solutions.

A time resolved fluorescence spectrophotometer (Edinburgh Instruments FSP920) was utilized to perform fluorescence lifetime experiments. Working condition was maintained at 25 °C and results were recorded at an excitation wavelength of 290 nm LED and 375 nm Laser Diode using a cuvette having path length 1 cm. In all the cases, the sample is repetitively excited using a pulsed light source with a repetition rate of 10-MHz and a 1-ns FWHM. The emission polarizer was vertical. The lifetime data were calculated by software with fixed fitting range. The time correlated single photon counting (TCSPC) method was used to calculate the lifetime data. The life time data (Global Analysis) were calculated by the software package with fitting range 205–4000 channels.

All the experiments were done four times. The experimental errors were found within 1–2 nm. The experimental standard errors were calculated based the following equations for four consecutive run for the same experiment at same condition.

$$SD = \sqrt{\sum_{i=1}^n \frac{1}{n-1} (x - \bar{x})^2} \quad (1)$$

where SD is standard deviation, x is individual data points, \bar{x} is the mean value of the experiments and n is the total number of observations. The standard error (SE) was measured by sample standard deviation obtained divided by the square root of number of observations

$$SE = \frac{SD}{\sqrt{n}} \quad (2)$$

The experimental errors in wavelength for both the UV–vis and fluorescence measurement were found to be in the range of 1–2 nm. Error in Quantum yield calculation lies in the range of 8–10%. The experimental error for lifetime measurement lies between ± 0.5 ns range.

5.4.3. Study of circular dichroism spectra

CD spectra were recorded using a CD spectrometer with a cell path length of 1 mm at in different solvent at room temperature and variable temperature. All the samples were with 50 μM concentration and prepared in spectroscopic grade solvents.

5.4.4. Macromodel study

Next, MD simulations for the pentapeptides were carried out with Schrödinger Macromodel (Maestro vs. 9.1) software package using an OPLS 2005 force field. The starting structures for the were the global minimum conformers.

Acknowledgements

The authors thank DBT, [BT/PR5169/BRB/10/1065/2012 and BT/PR5169/ BMB/2015/39] Govt. of India., for financial support.

Appendix A. Supplementary data

Supplementary material related to this article can be found, in the online version, at doi:<https://doi.org/10.1016/j.jphotochem.2019.04.024>.

References

- [1] K.E. Sapsford, L. Berti, I.L. Medintz, Materials for fluorescence resonance energy transfer analysis: beyond traditional donor-acceptor combinations, *Angew. Chem. - Int. Ed.* 45 (28) (2006) 4562–4588, <https://doi.org/10.1002/anie.200503873>.
- [2] (a) P.R. Selvin, Fluorescence resonance energy transfer, *Methods Enzymol.* 246 (1995) 300–334; (b) J.R. Lakowicz, *Principles of Fluorescence Spectroscopy*, 2nd ed., Kluwer Academic/Plenum, New York, 1999.
- [3] E. Haas, M. Wilchek, E. Katchalski-katzir, I.Z. Steinberg, Distribution of end-to-end distances of oligopeptides in solution as estimated by energy transfer (Fluorescence Decay/Conformation), *PNAS* 72 (5) (1975) 1807–1811.
- [4] (a) I.C. Yeh, G. Hummer, Peptide loop-closure kinetics from microsecond molecular dynamics simulations in explicit solvent, *J. Am. Chem. Soc.* 124 (23) (2002) 6563–6568, <https://doi.org/10.1021/ja025789n>; (b) D. Roccatano, W.M. Nau, M. Zacharias, Structural and dynamic properties of the CAGQW peptide in water: a molecular dynamics simulation study using different force fields, *J. Phys. Chem. B* 108 (48) (2004) 18734–18742, <https://doi.org/10.1021/jp0475077>.
- [5] (a) Michael G. Erickson, Daniel L. Moon, D.T. Yue, DsRed as a FRET partner with EGFP and ECFP - poster, *Biophys. J.* 80 (1a) (2001) 1520; (b) G.H. Patterson, D.W. Piston, B.G. Barisas, Forster distances between green fluorescent protein pairs, *Anal. Biochem.* 284 (2) (2000) 438–440; (c) B.A. Pollok, R. Heim, Using GFP in FRET-based applications, *Trends Cell Biol.* 9 (2) (1999) 57–60; (d) C. Badorff, N. Berkely, S. Mehrotra, J.W. Talhouk, R.E. Rhoads, K.U. Knowlton, Enteroviral protease 2A directly cleaves dystrophin and is inhibited by a dystrophin-based substrate analogue, *J. Biol. Chem.* 275 (15) (2000) 11191–11197.
- [6] H. Sahoo, W.M. Nau, Phosphorylation-induced conformational changes in short peptides probed by fluorescence resonance energy transfer in the 10 Å domain, *ChemBioChem* 8 (5) (2007) 567–573.
- [7] (a) A. Iqbal, S. Arslan, B. Okumus, T.J. Wilson, G. Giraud, D.G. Norman, T. Ha, D.M.J. Lilley, *PNAS* 105 (2008) 11176–11181; (b) S.S. Vogel, T.A. Nguyen, B.W. van der Meer, P.S. Blank, *PLoS One* 7 (2012) e49593 and references therein; (c) T.S. Blacker, W.Y. Chen, E. Avezov, R.J. Marsh, M.R. Duchon, C.F. Kaminski, A.J. Bain, Investigating state restriction in fluorescent protein FRET using time-resolved fluorescence and anisotropy, *J. Phys. Chem. C Nanomater. Interfaces* 121 (2017) 1507–1514 and references therein; (d) M. Millington, G.J. Grindlay, K. Altenbach, R.K. Neely, W. Kolch, M. Bencina, N.D. Read, A.C. Jones, D.T.F. Dryden, S.W. Magennis, High-precision FLIM-FRET in fixed and living cells reveals heterogeneity in a simple CFP-YFP fusion protein, *Biophys. Chem.* (2007) 1273155–1276410.
- [8] Y. Xu, M.S. Hixon, P.E. Dawson, K.D. Janda, Development of a FRET assay for monitoring of HIV Gp41 core disruption, *J. Org. Chem.* 72 (18) (2007) 6700–6707.
- [9] (a) S.S. Bag, S. Jana, A. Yashmeen, S. De, Triazolyl-β-Aza-e-amino acid and its aromatic analogue as novel scaffolds for β-Turn peptidomimetics, *Chem. Commun.* 51 (25) (2015) 5242–5245; (b) S.S. Bag, A. Yashmeen, Uracil-amino acid as a scaffold for β-sheet peptidomimetics: study of photophysics and interaction with BSA protein, *Bioorg. Med. Chem. Lett.* 27 (24) (2017) 5387–5392; (c) S.S. Bag, S. Jana, M.K. Pradhan, Synthesis, photophysical properties of triazolyl-donor/acceptor chromophores decorated unnatural amino acids: incorporation of a pair into Leu-Enkephalin peptide and application of triazolylperylene amino acid in sensing BSA, *Bioorg. Med. Chem. Lett.* 24 (16) (2016) 3579–3595; (d) S.S. Bag, S. Jana, A. Yashmeen, K. Senthilkumar, R. Bag, Triazolyl-donor-acceptor chromophore-decorated unnatural amino acids and peptides: FRET events in a β-Turn conformation, *Chem. Commun.* 50 (4) (2014) 433–435.
- [10] (a) B. Rubinov, N. Wagner, H. Rapaport, G. Ashkenasy, Self-replicating amphiphilic β-Sheet peptides, *Angew. Chem. - Int. Ed.* 48 (36) (2009) 6683–6686; (b) K.Y. Tsang, H. Diaz, N. Graciani, J.W. Kelly, Hydrophobic cluster formation is necessary for dibenzofuran-based amino acids to function as β-Sheet nucleators, *J. Am. Chem. Soc.* 116 (9) (1994) 3988–4005;

- (c) A. Fujii, Y. Sekiguchi, H. Matsumura, T. Inoue, W.S. Chung, S. Hirota, T. Matsuo, Excimer emission properties on pyrene-labeled protein surface: correlation between emission spectra, ring stacking modes, and flexibilities of pyrene probes, *Bioconjug. Chem.* 26 (3) (2015) 537–548;
- (d) M.L. Tiffany, S. Krimm, Circular dichroism of the “Random” polypeptide chain, *Biopolymers* 8 (3) (1969) 347–359.
- [11] (a) K. Oh, Z. Guan, A convergent synthesis of new β -turn mimics by click chemistry, *Chem. Commun. (Camb.)* 3 (29) (2006) 3069–3071;
- (b) H. Kessler, Conformation and biological activity of cyclic peptides, *Angew. Chem. Int. Ed. Engl.* 21 (7) (1982) 512–523;
- (c) S.H. Gellman, G.P. Dado, G.B. Liang, B.R. Adams, Conformation-directing effects of a single intramolecular amide-amide hydrogen bond: variable-temperature NMR and IR studies on a homologous diamide series, *J. Am. Chem. Soc.* 113 (1991) 1164–1173;
- (d) N.J. Baxter, M.P. Williamson, Temperature dependence of ^1H chemical shifts in proteins, *J. Biomol. NMR* 9 (1997) 359–369.
- [12] (a) MacroModel, MacroModel Version 9.9, Schrodinger, New York, 2012;
- (b) A. Feher-Voelger, J. Borges-Gonzalez, R. Carrillo, E.Q. Morales, J.G.-P.T. Martin, Synthesis and conformational analysis of cyclic homooligomers from pyranoid *e*-sugar amino acids chem, *Eur. J.* (2014), pp. 4007–4022.
- [13] (a) M.A. Rizzo, G.H. Springer, B. Granada, D.W. Piston, An improved cyan fluorescent protein variant useful for FRET, *Nat. Biotechnol.* (2004) 224445–244910;
- (b) J.W. Borst, M.A. Hink, A. van Hoek, A.J.W.G. Visser, Effects of refractive index and viscosity on fluorescence and anisotropy decays of enhanced cyan and yellow fluorescent proteins, *J. Fluoresc.* (2005) 152153–156010;
- (c) S.T. Hess, E.D. Sheets, A. Wagenknecht-Wiesner, A.A. Heikal, Quantitative analysis of the fluorescence properties of intrinsically fluorescent proteins in living cells, *Biophys. J.* (2003) 8542566–9258010.
- [14] (a) S. Lindhoud, A.H. Westphal, C.P. van Mierlo, A.J. Visser, J.W. Borst, Rise-time of FRET-Acceptor fluorescence tracks protein folding, *Int. J. Mol. Sci.* 15 (2014) 23836–23850.